Ann. Rev. Astron. Astrophys. 1986. 24 : 329–75

THE EVOLUTION OF MASSIVE STARS WITH MASS LOSS

Cesare Chiosi

Institute of Astronomy, vicolo Osservatorio 5, 35122 Padova, Italy

André Maeder

Geneva Observatory, CH-1290 Sauverny, Switzerland

1. INTRODUCTION

During their evolution, massive stars partly evaporate by stellar winds, as shown by UV spectroscopy from the *Copernicus* and *IUE* satellites. The study of mass loss in stellar evolution has greatly improved our understanding of the properties of massive stars, and several major consequences have been found to result from evolution with mass loss. Firstly, the tracks in the HR diagram are substantially changed by mass loss, and thus the genetic relationships between OB stars, Hubble-Sandage variables, blue and red supergiants, and Wolf-Rayet (WR) stars are clarified. This is a necessary step for understanding the differences between the distributions of massive stars in galaxies. Secondly, as a result of the removal of stellar envelopes by mass loss, the products of nucleosynthesis appear at the stellar surface, where they are spectroscopically observable and thus offer a new test of stellar evolution. The wind ejecta also contribute to galactic enrichment as well as to cosmic-ray injection. Thirdly, the effects of mass loss on the internal structure of massive stars influence the nature of supernovae precursors and their chemical yields, as well as the general stellar stability throughout evolution.

We interpret "massive stars" to be those stars with an initial mass larger than about 9 $M_{\odot}$ at the beginning of the hydrogen-burning phase. Such stars experience other stages of quiet nuclear burning after the H- and He-burning phase. In less massive stars (so-called intermediate-mass stars) an electron-degenerate carbon-oxygen core forms after the He phase, and

0066–4146/86/0915–0329$02.00

undergoes explosive carbon ignition. The evolution of intermediate-mass stars has been reviewed by Iben & Renzini (120, 121). Other recent reviews on massive star evolution are those by Chiosi (51, 52, 54), Humphreys (113, 114), de Loore (145–147), and Maeder (161, 168, 169). The supernova explosions of massive stars have been discussed by Nomoto (199) and Woosley et al. (272).

2. EVOLUTION AT CONSTANT MASS

We start by recalling the main results of constant-mass evolution, to which models with mass loss are frequently compared. Constant-mass evolutionary models of massive stars are affected by the uncertainty of semiconvective instability, whose essential nature was first recognized by Schwarzschild & Härm (226). In brief, the existence of semiconvection is due to the fact that radiation pressure and electron scattering dominate pressure and opacity in massive stars. As a consequence of the high radiation pressure, the convective core tends to be larger at higher masses and to expand as the star evolves, causing a chemical discontinuity to occur at the expanding border of the core. Such a discontinuity would cause no difficulty if the opacity were dominated by Kramers bound-free terms, but with dominant electron scattering, it soon becomes evident that radiative equilibrium outside the external border of the formal convective core cannot be established. The difficulty is removed by assuming that as the core increases by a small amount into the radiatively stable zone, a partial mixing takes place tending to equalize the temperature gradient to the adiabatic value ($\nabla_T = \nabla_{TA}$, hereafter referred to as the neutrality condition). This neutrality condition was criticized by Sakashita & Hayashi (216, 217), who argued that in the presence of a molecular weight gradient, the density gradient should be equal to the adiabatic value ($\nabla_\rho = \nabla_{\rho A}$), as proposed by Ledoux (143).

The basic mechanism for semiconvective mixing is unknown, however. Kato (126) pointed out that the density condition must be applied in a medium with a gradient in molecular weight when thermal dissipation is neglected. If, however, the medium is thermally dissipative, the temperature condition is recovered owing to the onset of oscillatory convection, whose growth time is short enough to ensure that the temperature condition is satisfied. But Kato's analysis is a local one, whereas a correct stability analysis should take into account the whole star (or in other words, the effects of external, stabilizing radiative zones). This problem was investigated by Gabriel (92), Auré (18), and Gabriel & Noels (93). The latter authors recognized the ultimate physical cause of semiconvection in the vibrational instability of gravity modes of high surface spherical

harmonic (with growth time of the order of 10^3–10^4 yr) trapped in the region with a gradient in molecular weight. Gabriel & Noels (93) also argued that as a result of the instability, the temperature gradient is reduced to a value close to the adiabatic one. Uncertainties concerning the validity of the two neutrality conditions led to a large number of possible stellar models and a flurry of arguments supporting both conditions. Relevant contributions to the subject were the papers by Chiosi & Summa (61), Simpson (231), Stothers (240), Stothers & Chin (241), Varshawsky & Tutukov (264), and Ziolkowski (174).

Numerous calculations have shown that semiconvection (whatever the adopted neutrality condition) does not greatly affect the stellar structure during the main-sequence phase. However, during the shell H-burning and He-burning phases, semiconvection plays a significant role, and the evolutionary results are dependent on the adopted criteria and the input physics of model construction. We report here only on the major results and refer the reader to the reviews by Chiosi (49), Dallaporta (75), Iben (119), de Loore (145), and Massevich & Tutukov (177) for more details.

The lower limit on the mass leading to differences in the evolution between the temperature and the density criteria is about 13 $M_\odot$. The density condition leads to the onset of a shallow gradient in chemical composition, which is not modified during the shell H-burning phase; thermal equilibrium in the models is restored only after they have undergone envelope expansion up to the Hayashi line (red supergiant stages). Subsequent evolution takes place either in the same region of the HR diagram or in extended loops. When the temperature condition is used, the onset of the H-burning shell causes a fully convective zone to develop in the region of intermediate instability, with consequent change in the chemical profile. In the mass range 13–50 $M_\odot$, core He-burning takes place (as a result of the plateau-shaped chemical profile) either entirely in the blue supergiant region (135, 163) or partly in the blue and partly in the red supergiant zone (61). In any case, the evolution proceeds from blue to red, and the time spent in the red supergiant region is very short or even negligible (cf. 135, 241).

The above scheme does not hold for both lower and higher masses, although for different reasons. Lower mass stars, independent of the neutrality condition, start core He burning as red supergiants and perform a loop in the HR diagram. On the other hand, stars with a mass greater than about 50 $M_\odot$, independent of the neutrality criterion, start and spend their whole core He-burning phase as red supergiants; these stars, however, could loop across the HR diagram if their H-burning shell moves outward in mass enough to reach the jump in chemical composition caused by the intermediate and/or external full convection before it reaches the stage of

central He exhaustion (274). This, if it occurs in stars of lower mass once they have been pushed toward the Hayashi line by the density criterion, is unlikely to occur in very massive stars, which therefore remain as red supergiants over the whole core He-burning phase.

The regions of stationary nuclear burning resulting from a large body of evolutionary computations are schematically shown in Figure 1, together with the HR diagram for supergiant stars in the solar vicinity [from Humphreys & McElroy (116)]. Similar HR diagrams for galactic and Magellanic Clouds supergiants can be found in Humphreys (113, 114). It is evident that models of massive stars evolved at constant mass cannot

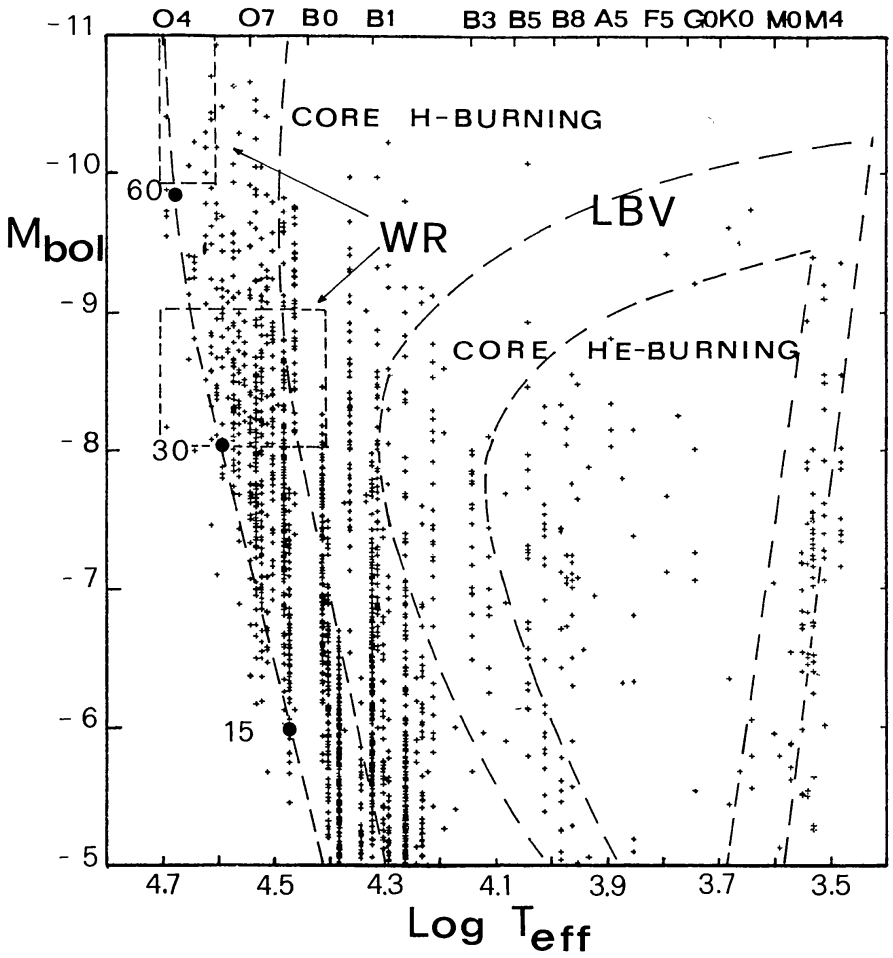

Figure 1 The HR diagram (M_{bol} vs log T_{eff}) for stars in clusters and associations in the solar vicinity [from Humphreys & McElroy (116)]. The top scale shows the relationship between effective temperature and spectral type. The areas corresponding to core H- and He-burning phases of constant-mass models with typical Pop I chemical composition ($X = 0.700$, $Z = 0.020$) are indicated. The locations of the 15-, 30-, and 60-$M_{\odot}$ stars on the zero-age main sequence are also shown. In addition, we schematically indicate the position of WR and luminous blue variable (LBV) stars.

reproduce the observed distribution of luminous stars, together with their number frequency per spectral type. In fact, while the theoretical main-sequence band (locus of core H-burning stars) is expected to widen at increasing luminosity, observations indicate a steady decline of the luminosity with decreasing effective temperature ($T_{\rm eff}$). Core He-burning models seem too cool to represent the bulk of blue supergiants and predict too many red supergiants of very high luminosity. (Indeed, on the contrary, no such stars are seen.) Finally, in the mass range of about 20–50 $M_{\odot}$, the models evolved at constant mass predict almost no red supergiants, whereas there are many such stars observed.

3. DIAGNOSTICS OF STELLAR WINDS AND MASS LOSS RATE PARAMETERIZATIONS

It is now recognized that mass loss is a common feature of all stars of high luminosity: OV stars, Of stars, OB giants and supergiants, M giants and supergiants, and WR stars. However, the scale of mass loss varies greatly both with the type of star and with luminosity. Ideally, we would like to know, either from observation or theory, the mass-loss rate $\dot{M}$ and the ejection velocity as functions of basic stellar parameters (luminosity, mass, radius, chemical composition, etc). It would then be possible to incorporate these functions in evolutionary models. We are also interested in the physical mechanism by which mass is ejected from stars. The observational evidence of this phenomenon has been recently reviewed by Barlow (21), Cassinelli (41), Conti (65, 67), Dupree (85), Kwok (133), and de Loore (148). The theoretical aspects of this subject have been amply discussed by Abbott (7), Castor (43), Hearn (104), and Linsky (144).

3.1 *Mass Loss from Early-Type Stars and WR Stars*

Mass loss from OB supergiants is detected by the presence of broad P Cyg profiles of C IV and Si IV lines indicating that the material is expanding at about 2000 km s^{-1}, well in excess of the escape velocity of about 600 km s^{-1}. Lucy & Solomon (155) first recognized that in luminous early-type stars, material is driven outward by the gradient of radiation pressure on resonance lines of dominant elements. Subsequently, Castor et al. (44) extended the theory to lines of less abundant elements and also explained quantitatively the observed mass loss rates. The radiation pressure theory has been greatly improved by Abbott (1–7), to whom we refer for a thorough discussion of the present status of the theory. Although the radiation pressure theory is by far the most developed of all the models available (as it makes predictions about $\dot{M}$), its main drawback is its

inability to predict the X-ray emission that is observed for OB stars. Ways out of this difficulty have been proposed by Nelson & Hearn (192) and Lucy & White (156).

Another theory for describing mass loss is the fluctuation theory of Andriesse (9–11), which rests on the concept of thermodynamic fluctuations and partial equilibrium in a star. These fluctuations are supposed to act as an input of energy to the atmosphere, leading to a stochastically steady ejection of matter in the form of a wind. The Andriesse theory also makes predictions about the dependence of the mass loss rate on stellar parameters.

The last set of models consists of those that predict some form of mechanical input to the wind via the formation of a corona. These models include the warm-wind coronal theory of Lamers & Rogerson (140), the cool-wind thin corona model of Cassinelli et al (42), and the nozzle model of Cannon & Thomas (38). Simple predictions of $\dot{M}$ are not yet possible with this group of wind models.

There are several methods for determining the mass loss rates. In the visible and UV, P Cyg and emission lines (Hα, He II 4686) can be used, whereas in the radio and infrared, the determinations are based on free-free emission. The radio technique, in particular, was recognized as the most accurate means of measuring the mass loss rate, since the observed radio emission originates from the external regions of the circumstellar envelope where the outflow has already reached the terminal velocity. Another powerful diagnostic of mass loss is the UV technique, since many strong atomic resonance lines are located in the UV region. In this case also, accurate determinations of the terminal velocities are possible. This is particularly useful in combination with radio measurements, because the latter can only provide the ratio $\dot{M}/v_\infty$ and not $\dot{M}$ itself. The reader is referred to the reviews by Abbott (7), Kwok (133), and de Loore (148) for more details.

The large number of stars observed with *IUE* and radio techniques allows statistical analyses to be performed to assess the dependence of the mass loss rate on basic stellar parameters (luminosity, radius, mass, and metallicity). Mass loss rates for early- and late-type stars (see below) as a function of luminosity are shown in Figure 2. The diagram shows the data sampled by de Jager et al. (124) from the literature for stars with known luminosity, effective temperature, and mass loss rate. The mass loss rates for OB stars increase with the luminosity, although a large spread in $\dot{M}$ exists at any given luminosity. Of stars have rates higher than normal OB type stars. WR stars in particular have nearly the same rates, which happen to be among the highest values observed in early-type stars (21). The

physical cause of such an increase in the mass loss rates for WR stars has not yet been explained.

Essentially two types of parameterization for $\dot{M}$ have been proposed. A first simply correlates the mass loss rate to the stellar luminosity ($\dot{M} = aL^b$) and a second type assumes $\dot{M}$ to depend on luminosity, mass, and radius ($\dot{M} = \alpha L^\beta M^\gamma R^\delta$). An overview of the existing formulations for the mass loss rate is presented in Table 1. Despite their similarity, the various

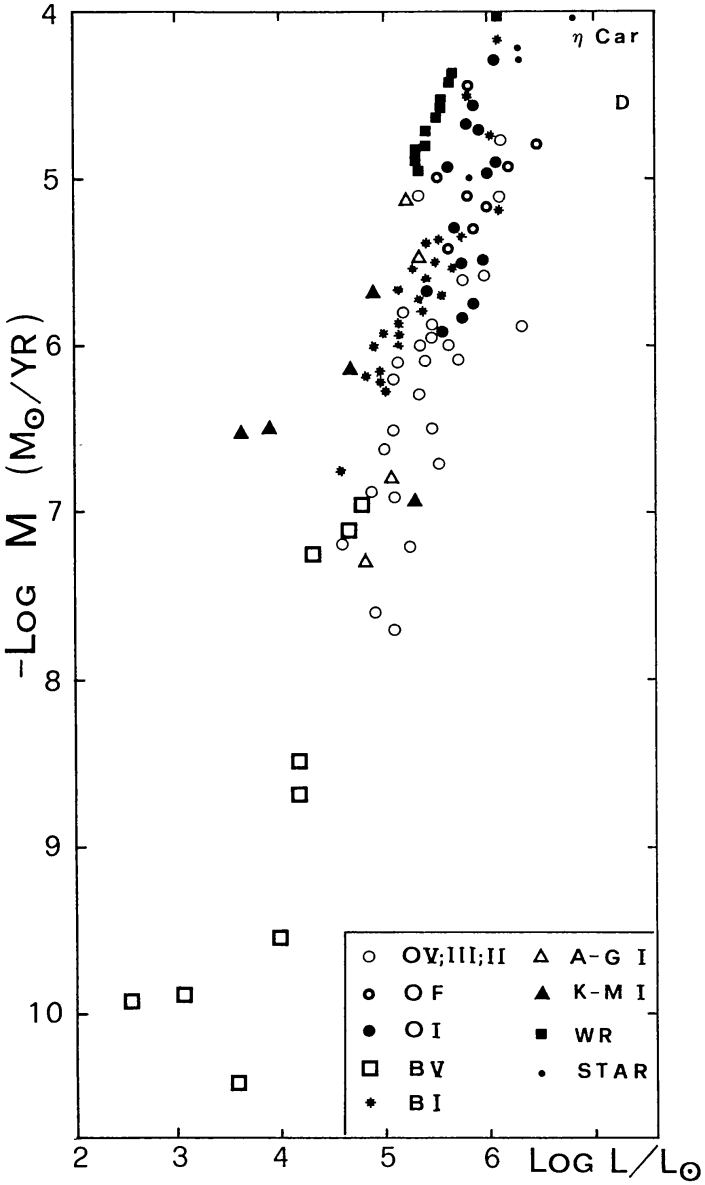

Figure 2 The relation between mass loss rate and luminosity for stars with known mass loss rate, luminosity, and effective temperature. The data are taken from the list of de Jager et al. (124). The meaning of the various symbols is shown in the bottom panel of the figure.

Table 1 Current mass loss rate parameterizations[a]

Radiation pressure theory	References
$\dot{M} = L/cv_{th}(\alpha/\Gamma)[(1-\alpha)/(1-\Gamma)]^{(1-\alpha)/\alpha}(K\Gamma)^{1/\alpha}$	
$\Gamma = \sigma_e L/4\pi GMc$	Castor et al. (44)
$\dot{M} = 1.4 \times 10^{-15}(L/L_\odot)^{1.98}(Z/Z_\odot)^{0.94}(M_{eff}/M_\odot)^{-1.03}(T_{eff}/10^4\ \mathrm{K})^{-0.02}$	
$M_{eff} = M(1-\Gamma)$	Abbott (5)
$\dot{M} = NL/c^2, \quad N = 100$–$300$	de Loore et al. (151)
Fluctuation theory	
$\dot{M} = (t_D/t_K)^{1/2}LR/GM$	Andriesse (9)

Empirical relations $\dot{M} = f(L)$	for O-Of-B stars
$\log \dot{M} = 1.10 \log L + \text{constant}$	Barlow & Cohen (22)
$\log \dot{M} = 1.56 \log L - 14.10$	Abbott et al. (8)
$\log \dot{M} = 1.50 \log L - 14.00$	de Loore (148)
$\log \dot{M} = 1.73 \log L - 15.80$	Garmany et al. (98)
$\log \dot{M} = 1.62 \log L - 14.97$	Garmany & Conti (95)

Empirical relations $\dot{M} = f(L, R, M, \ldots)$	for O-Of-B stars
$\log \dot{M} = 0.72 \log L + 2.5 \log [R/(1-\Gamma)M] - 9.59$	Chiosi (53)
$\log \dot{M} = 1.4 \log L + 0.06 \log R - 0.99 \log M - 15.3$	Lamers (136)
$\log \dot{M} = 1.75 \log L + \log [R/(1-\Gamma)M]$	Chiosi & Olson [1983; cf. Garmany & Conti (95)]
$\log \dot{M} = \log L + 0.8 \log R + 0.6 \log M - 13.36$	Garmany & Conti (95)
$\log \dot{M} = 1.3 \log L + 1.2 \log (v_\infty/v_{esc})$	Garmany & Conti (95)
$\log \dot{M} = \log (L/v_\infty) - 10.63$	Wilson & Dopita (270)

Empirical relations $\dot{M} = f(L, R, M, \ldots)$	all across the HR diagram
$\log \dot{M} = 1.07 \log L + 1.77 \log R - 14.3$	Waldron (265)
$\log \dot{M} = -a_1 - a_2 x - a_3 x^2 - a_4 x^3 - a_5 y - a_6 y^2 - a_7 y^3 - a_8 xy - a_9 x^2 y - a_{10} xy^2$	de Jager et al. (124)

$x = \log T_{eff} - 4$	$a_2 = 0.1104$	$a_3 = -0.4311$	$a_4 = 3.579$
$y = \log L - 5$	$a_5 = -1.571$	$a_6 = -0.0109$	$a_7 = -0.2175$
$a_1 = 6.3168$	$a_8 = -0.8381$	$a_9 = -1.2487$	$a_{10} = 1.5822$

Empirical relations	for red supergiants
$\log \dot{M} = \log \eta + \log [L/(gR)]$	Reimers (209)
$\log \dot{M} = \log \eta_{FR} + \log [L_a/(gR)]$	Fusi-Pecci & Renzini (91)
$\log \dot{M} = \log \varepsilon + \log [L_a/(v_{esc}v_s)]$	Chiosi et al. (60)
$\log \dot{M} = 1.3 \log L + \text{constant}$	Maeder (162, 163); Bertelli et al. (26)

[a] Note that $\dot{M}$ is in solar masses per year, and L, M, and R are in solar units. Notation as follows: v_{th}, thermal velocity; v_∞, terminal velocity; v_{esc}, escape velocity; L_a, acoustic luminosity.

relations are not strictly equivalent, and when used in evolutionary computations of massive stars, they lead to substantially different results. They may also be used to identify the mass loss mechanism itself, since often they have been advocated to defend or to reject one or another theory of mass loss. In fact, the original radiation pressure theory (44, 155) predicts the mass loss rate to linearly increase with the luminosity. This seemed to be confirmed by the empirical relation of Barlow & Cohen (22). Subsequently, however, Lamers et al. (138) and Conti & Garmany (70) pointed out that stars of the same luminosity show a large range in $\dot{M}$, which could not be accounted for by the original theory. In addition, the slope itself of the luminosity dependence was questioned. Although on the observational side the slope seemed to settle around the value 1.7 (cf. Figure 2), and the improved radiation pressure theory of Abbott (7) increased the slope to about 2 (cf. Table 1), the spread in $\dot{M}$ is still there even in the most recent studies (270). Perhaps the most important result of these observational determinations of $\dot{M}$ is the fairly convincing evidence of a systematic increase in $\dot{M}$ from OV to Of to WR stars.

3.2 *Mass Loss Rates From Late-Type Stars*

Red supergiant stars are known to lose mass at rates as high as those from early-type stars. Complete surveys of the optical, infrared, and radio data are given by Cassinelli (41), Goldberg (100), Kwok (133), Merrill (184), Moran (190), and Reimers (211, 212). Stellar winds from late-type giants and supergiants differ from their early-type counterparts in that they have two components (gas and dust), which interact both thermally and dynamically. Diagnostics of stellar winds in these objects come from circumstellar gas shells studied by Bernat (25), Hagen (102), Reimers (208–210), and Sanner (218). The major uncertainty in the derivation of a mass loss rate is in the size of the shell, whose radius ranges from about one stellar radius to 100 stellar radii and accordingly yields rates varying from 10^{-7} to $10^{-5}\ M_{\odot}\ \mathrm{yr}^{-1}$. The emission at 10 μm attributed to dust grains in a circumstellar shell is also used to estimate the mass loss rate. Finally, both the occurrence of stellar winds and estimates of the mass loss rates can be inferred from the ratio of the intensities of two peaks of emission in the Ca II K line, as well as from the Mg II lines (239) and UV, X-ray, and radio emission.

On the theoretical side, several models have been advanced to explain the rapid mass loss observed in cool stars. These can be grouped into four categories according to the powering mechanism: radiation pressure on dust grains (atoms and/or molecules); solar-type wind presumably driven by the pressure of hot gas; coronal-type models in which the wave pressure

rather than the gas drives the wind; and finally models in which mass loss is caused by shock waves. All of these models have been discussed by Castor (43), to whom we refer to for more details.

The most popular parameterization of the rates was advanced long ago by Reimers (209) on dimensional grounds. He suggested a formula of the form $\dot{M} = 4 \times 10^{-13}\eta L/(gR)$, where all quantities are in solar units and η ranges between 0.3 and 3. This formula has been amply used in conjunction with evolutionary computations. Another important formulation of the mass loss rate for cool stars is due to Fusi-Pecci & Renzini (91), and it is otherwise known as the "acoustic flux mechanism." They supposed that the acoustic energy generated in the convective outer layers of cool stars may power the winds of these stars. Following up on this idea, they expressed the rate of mass loss as $\dot{M} = \eta_{FR}L_a/(gR)$, where L_a is the acoustic luminosity and η_{FR} is an adjustable parameter. By imposing several astrophysical constraints not directly related to the wind mechanism itself, but mainly to the total amount of mass that has to be lost by low-mass red giants and by intermediate-mass late-type stars, Fusi-Pecci & Renzini (91) found that η_{FR} is the same in a wide range of astrophysical circumstances and has a value of 8×10^{-4}. The difficulties that made the acoustic flux theory questionable have been discussed by Goldberg (100). This formulation, however, has been used in the first study of the effect of mass loss all across the HR diagram for supergiant stars (60).

3.3 *Hot-Cool Star Connection*

In concluding this section, it seems advisable to comment on a point that may deserve further investigation and lead in the near future to a deeper understanding of the mass loss phenomenon—namely, the possible connection between hot and cool stars as far as mass outflow is concerned. Waldron (265), who collected data for some 300 stars of all spectral types and luminosities, suggested that the wind luminosity ($L_W = 0.5\dot{M}v_\infty^2$) correlates to the bolometric luminosity, and that the terminal velocity v_∞ correlates to the stellar effective temperature. From these two relationships, it follows immediately that a relation between the mass loss rate and the stellar luminosity and radius (or T_{eff}) exists. De Jager et al. (124) provided a general parameterization for $\dot{M}$ as a function of the stellar luminosity and T_{eff} for a large sample of stars of various spectral types and luminosities. Although the two final relationships are different in several details, both predict the same general trend for the mass loss rate across the HR diagram. Whether these findings are supportive of a deep hot-cool star connection as far as the stellar wind is concerned cannot yet be assessed.

4. EFFECTS OF MASS LOSS ON INTERNAL STRUCTURE AND EVOLUTION OF MASSIVE STARS

The realization that such large rates of mass loss are likely to exist in most luminous hot and cool stars stimulated many independent studies of the effects of mass loss on stellar evolution. Before describing the model results in detail, we note several considerations that are important in assessing the validity of these evolutionary scenarios.

1. The mass loss rates are customarily expressed by empirical formulations, which contain one or more free parameters scaling the mass loss rates until plausible evolutionary results are obtained.
2. The stellar mass is simply decreased with time according to the assumed mass loss rate; thus the tremendous task of self-consistency between the wind properties and the underlying stellar structure is avoided.
3. Such a way of proceeding does not always guarantee consistency between the mass loss rates assigned to an evolutionary phase and the type of stars from which the rates are derived. This may be particularly crucial for those stars that, although in different evolutionary phases, crowd the same area of the HR diagram.
4. The large body of evolutionary models computed so far makes evident that the model structure in each individual evolutionary phase is very sensitive to the past history of mass loss.

Recent reviews on this subject are by Chiosi (51, 52, 54), de Loore (145–147), and Maeder (168, 169), to whom we refer to for all details. In the following, we are concerned only with the main general results. These are based on the work of an impressive number of authors, including (listed in chronological order) Tanaka (252, 253), Hartwick (103), Simon & Stothers (230), Chiosi & Nasi (58), de Loore et al. (151), Dearborn & Eggleton (80), Dearborn et al. (79), Sreenivasan & Wilson (235), Chiosi et al. (60), de Loore et al. (152), Stothers & Chin (244), Dearborn & Blake (78), Czerny (74), Chiosi et al. (59), Stothers & Chin (246), Maeder (159, 160), Noels et al. (195), Maeder (162, 163), Stothers & Chin (247), Bressan et al. (32), Noels & Gabriel (196), Brunish & Truran (35, 36), Doom (81, 82), Sreenivasan & Wilson (236), Maeder (166), Bertelli et al. (26), and Sreenivasan & Wilson (237).

4.1 *The Core and Shell H-Burning Phases*

Evolutionary models in the core and shell H-burning phases have been calculated using some of the various relations for $\dot{M}$ reported in Table 1.

In most models, similar effects of mass loss have been recognized. These are physically connected as follows:

1. The progressive reduction of the stellar mass makes the central temperature increase less rapidly than for constant-mass evolution; thus the mass of the convective core decreases more rapidly as evolution proceeds. However, the core mass fraction is larger in a star evolving with mass loss.

2. As a result of the smaller core, the luminosity of stars evolving with mass loss is lower than for constant-mass evolution. However, the star is always overluminous for its mass. As a consequence of the lower luminosity, the extension of semiconvection and/or intermediate full convection at the top of the H-burning shell is much smaller than in constant-mass models. The reduction is proportional to the mean mass loss rate. This fact makes less important the whole problem of semiconvective instability, one of the major uncertainties in the structure of massive stars. However, since this phenomenon is not definitely suppressed by mass loss unless very high rates are used, an accurate treatment of the chemical structure of these intermediate layers is still required. In fact, the chemical profile set up by intermediate convective instability (when it occurs) is one of the parameters controlling subsequent evolution, even in occurrence of mass loss.

3. As a result of the lower luminosity, the main sequence lifetime is somewhat increased by mass loss. Two competing effects can intervene: Both the smaller convective core and the lack of sufficient semiconvective feeding (leading to less fuel to burn) would shorten the lifetime. But this trend is weaker than that of the lower luminosity, and thus the net effect is an increase in the main sequence lifetime with increasing mass loss rate. The lifetime of the various nuclear stages of sequences evolved under typical mass loss rates are reported in Table 2.

4. For moderate mass loss, there is a slight main sequence widening as a result of the larger core mass fraction. In the case of heavy mass loss (i.e. loss sufficient to expose nuclearly processed material at the surface during main sequence evolution), there is also a main sequence narrowing due to the lower surface hydrogen content.

5. In order to readily interpret the results of many evolutionary computations under a variety of rates, simple analytical formulations in terms of basic stellar quantities have been advanced. According to Dearborn et al. (79), the numerical results can be organized in a simple scheme regulated by the parameter $\xi = t_{\rm H}\dot{M}/M$, where $t_{\rm H}$ is the core H-burning lifetime. For ξ below some critical value (0.25), the inclusion of mass loss does not change too much the behavior of the models. If ξ is greater than a limit of about 0.4 to 0.6 (depending on initial mass), the models become almost bare He cores embedded in a very thin H-deficient envelope. Mass loss in

Table 2 Luminosities and lifetimes (in units of 10^6 yr)[a]

Initial mass ($M/M_\odot$)	Log $L/L_\odot$	H-burning lifetime	He-burning lifetime	Fraction of He phase at log $T_{\rm eff} > 4.2$ (%)	Fraction of He phase at log $T_{\rm eff} < 3.8$ (%)
15	4.25	11.582	2.344	1	55
25	4.85	6.624	1.222	16	38
40	5.34	4.530	0.856	58	14
60	5.70	3.708	0.707	93	0
85	5.98	3.253	0.760*	100	0
120	6.23	2.810	0.840*	100	0

[a] The He phase is defined here as the phase extending from central H exhaustion to He exhaustion. The He phase is calculated using the $^{12}C(\alpha,\gamma)^{16}O$ cross section of Kettner et al. (127), except where noted by an asterisk, where the rates of Fowler et al. (89) have been used. The long He lifetimes for these two cases result from the strong decline of luminosity in the WR stage.

this case prevents models from expanding their envelopes any further, so they remain forever at high effective temperatures and tend toward a quasi-homogeneous state in which the surface composition is close to the central value. However, since very large rates ($\dot{M} > 4 \times 10^{-5}\ M_\odot\ {\rm yr}^{-1}$ for an initial mass of 100 $M_\odot$, and $\dot{M} > 8 \times 10^{-6}\ M_\odot\ {\rm yr}^{-1}$ for an initial mass of 20 $M_\odot$) are required to reach this state, it seems unlikely that such a case may actually occur in real stars losing mass at the observed rates.

6. Mass loss changes the shape of isochrones and lines of constant mass in the HR diagram (60, 151). When mass loss is taken into account, lower ages are implied for a given luminosity and spectral type of a cluster turn-off point. The effect ranges from 0.5 to 1.5×10^6 yr at increasing mean mass loss rate (60). On the other hand, Paerels et al. (203) considered the effect to be negligible. The lines of constant mass are steeper than those of classical models, which leads to a systematic variation in the mass determined by means of evolutionary tracks. The problem is marginal for less massive and/or scarcely evolved stars, but it becomes severe for very massive and/or highly evolved stars (60).

7. The mass of the He core at the end of the core H-burning phase is smaller, and the chemical structure of the models shallower, than in constant-mass stars. Finally, a tiny intermediate convective zone may develop on top of the H-burning shell when the temperature criterion against convection and moderate mass loss rates is used in the previous stages.

4.2 *The Core He-Burning Phase*

The core He-burning phase of model stars that have evolved with mass loss is characterized by an apparently erratic location in the HR diagram,

which eludes simple explanations. Indeed, this location is extremely sensitive to many structural properties; the numerical results are summarized below. Numerical experiments carried out to isolate the response of the model to variations of its basic parameters have suggested several criteria for blueward and/or redward movements in the HR diagram (51, 52, 87, 161, 163). Broadly speaking, we may distinguish four internally competing effects: (*a*) the classical mirror expansion that responds to core contraction (cf. 213 for a recent discussion); (*b*) the increasing size of the He core by outward shifting of the H-burning shell and the increasing size of the fractional mass of the He core by mass loss, which favors redward evolution up to some critical value and blueward evolution afterward (99); (*c*) the homogenization of the envelope by large intermediate convective zones, which (if present) tend to limit the increase in the stellar radius; (*d*) a large luminosity-to-mass ratio, which favors envelope expansion. In particular, point (*b*) is regulated by mass loss during the post–main sequence stages and, more precisely, at low effective temperatures. It is clear that several plausible evolutionary scenarios are generated by the competition between the various factors discussed above.

Many sets of models of massive stars predict a ratio t_{He}/t_H of the lifetimes in the helium- and hydrogen-burning phases of about 0.08 to 0.13 (e.g. 36, 60, 135, 163, 246). However, there is an appreciable scatter in the predicted He-burning lifetimes, depending on mass-loss rates and other model assumptions. The t_{He}/t_H ratio in Table 2 amounts to about 0.19 for stars in the range of initial masses between 15 and 60 $M_\odot$ (171); similarly, Dearborn & Blake (78) obtained for a 30 $M_\odot$ model a t_{He}/t_H ratio of about 0.17. High mass loss rates in the WR stages, which lead to a lower luminosity, may increase the t_{He}/t_H ratio to 0.2 or 0.3, as in the case of the 85 and 120 $M_\odot$ models in Table 2. The He lifetime may also change with stellar opacities and nuclear reaction rates; in particular, the $^{12}C(\alpha,\gamma)^{16}O$ rate has been recently increased (127) by a factor of 3 to 5 with respect to the standard value (89). Other properties, such as the size of the convective core, the location and size of the H-burning shell, and even the treatment of the external layers (171), may influence the central conditions and in turn the He-burning lifetimes. We note that the observations favor rather large values of the t_{He}/t_H ratios, as shown in Sections 5.1 and 8.3 below.

A typical HR diagram for massive stars evolved with mass loss under plausible mass loss rates during core H- and He-burning phases is shown in Figure 3 (171). Similar diagrams (although constructed with somewhat older rates) can be found in Chiosi (51, 52, 54) and Maeder (163). It is appropriate to distinguish between three different mass ranges. The exact mass limits depend, however, on the adopted mass loss rates.

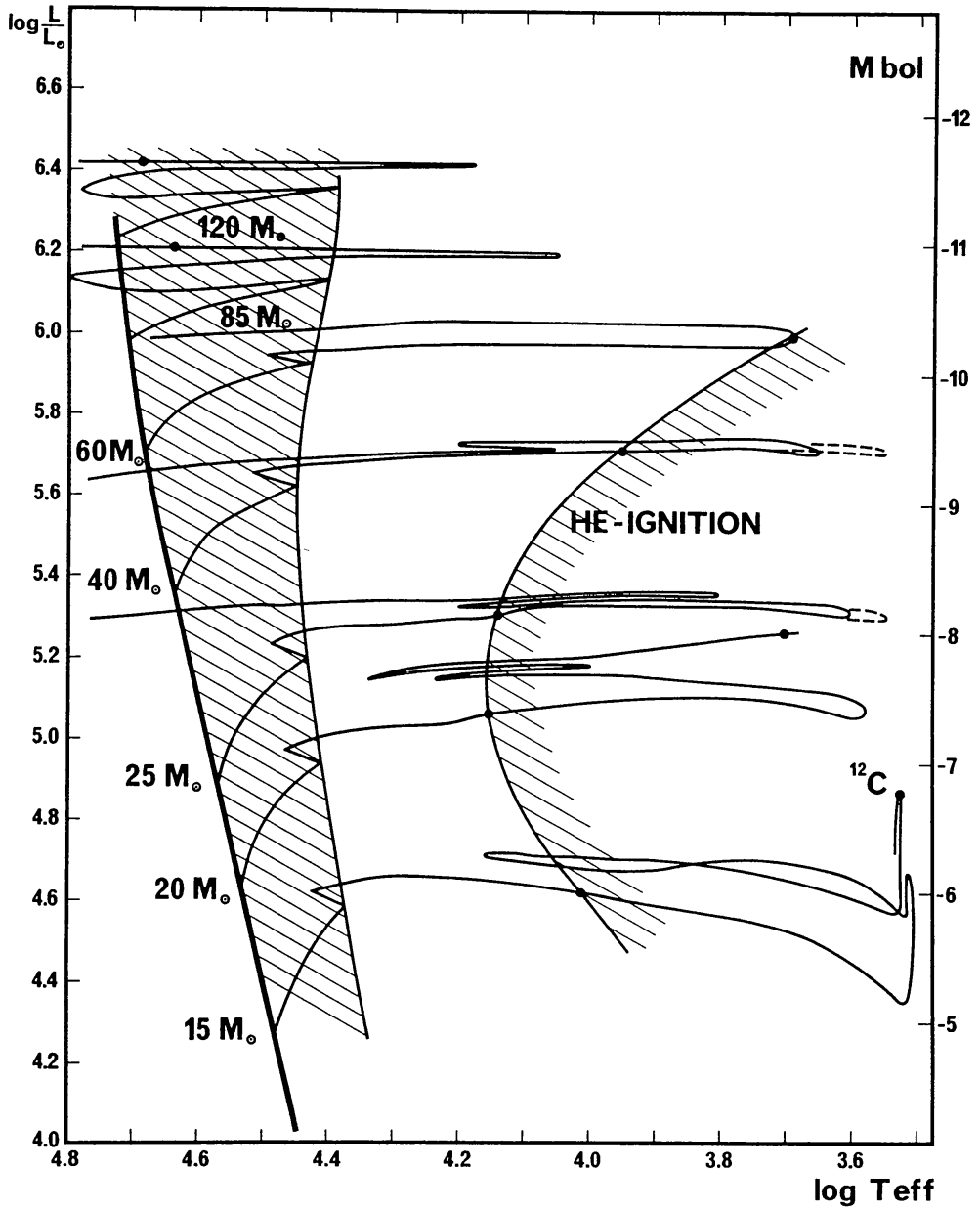

Figure 3 Evolutionary tracks in the HR diagram of massive stars with initial composition $X = 0.73$, $Z = 0.02$ evolved with mass loss by stellar winds. The hatched areas indicate the main sequence band and the beginning of He-burning, which is spent according to the repartition given in the last two columns of Table 2. The first dot along each track indicates the beginning of the He-burning phase. The second dot (if present) indicates the beginning of the C-burning phase. The mass loss rates for OB stars are from Garmany et al. (98); for red supergiants, the expression by Schönberner (225) scaled on the results by van der Hucht et al. (112) is used; and for WR stars, results by Barlow et al. (24) and Nussbaumer et al. (202) are adopted. These models were computed with Schwarzschild's criterion for convection and no convective overshooting. The evolutionary tracks indicated by the solid lines have been computed with mixing length in the outer convection equal to 0.3 × density scale height (171). The dashed lines show the effect of a different treatment of the outer convection (that is, of a mixing length equal to 1.5 × pressure scale height).

INITIAL MASSES LARGER THAN 60 $M_\odot$ The winds responsible for peeling during the main-sequence and early shell-H-burning phases are high enough to remove all stellar outer layers, leaving a bare He core. This prevents any evolution toward the red supergiant stage, and therefore the stars always keep on the left half of the HR diagram [see effect (*b*) above]. Zones that were initially in the core are exposed at the stellar surface, where they lead to large spectroscopically observable changes of chemical abundances. During the blue supergiant phase, these stars are located in the region of the luminous blue variables (LBV), also called Hubble-Sandage objects (see Figure 1). Such an identification is somewhat confirmed by spectroscopic observations (cf. Section 7.1). As a result of the very high mass loss rates [of the order of $10^{-3}\ M_\odot\ \mathrm{yr}^{-1}$ or more (137)], the remaining part of the envelope is ejected and the star evolves directly as a bare core, likely identifiable as a WR star. Observational evidence for such an evolutionary connection is given by P Cygni (139) and R127 (238). The origin of the extreme mass loss rates and light variations of LBV stars has been discussed by Stothers & Chin (249), who examined seven possible mechanisms. Two other processes, possibly responsible for violent recurrent outbursts of LBV stars, have also been recently proposed:

1. *Effects of turbulent pressure*. The extreme supergiants (even blue or yellow) possess a deep external convective zone due to the high radiation pressure (159). As evolution proceeds to the right, convection becomes almost supersonic and the dissipation of mechanical flux produces a gradient in turbulent pressure that leads to an outward acceleration (122, 123). Somewhere in the HR diagram, the resulting gravity vanishes. We call this the de Jager limit. It places an insuperable barrier to the redward hydrostatic evolutionary tracks. In the vicinity of this limit, enhanced mass loss could occur with recurrent relaxation oscillations. Model computations (166) show that a shell ejection is likely to occur with consequent large changes in T_{eff} and no luminosity variations; this corresponds well to observations by Appenzeller & Wolf (13). The large variability in visual magnitude is thus due to changes in bolometric corrections. The periodicity and exact nature of the oscillations responsible for successive shell ejections have yet to be clarified (cf. 14). Subsequent evolution of these stars is likely to correspond to the WR stage.

2. *Mass loss instability*. As emphasized by Appenzeller (15), radiatively driven winds can become dynamically unstable if a random increase of the wind results in an increase of the radiative acceleration g_{rad}. Indeed, the resulting total gravity is expressed as

$$g_{\mathrm{tot}} = g_{\mathrm{grav}}(1 - g_{\mathrm{rad}}/g_{\mathrm{grav}} - \ldots).$$

For a star evolving at constant luminosity, the gravity g_{grav} scales like T_{eff}^4. Now, if g_{rad} increases with T_{eff} less rapidly than T_{eff}^4, a decrease of T_{eff} leads to a higher g_{rad}/g_{grav} ratio, and thus to a lower g_{tot}. This in turn leads to an increase in the mass loss rate $\dot{M}$. This enhanced $\dot{M}$, as a result of the larger optical depth of the flow, reduces T_{eff}, which again increases $\dot{M}$ and leads to violent shell ejection, as proposed by Appenzeller (15). Detailed atmosphere models are necessary to predict g_{rad}. From the existing calculations, g_{rad} grows slower than T_{eff}^4 in the range of log T_{eff} (from about 4.08 to 4.28), which gives rise to an instability strip. The recurrent shell ejections from LBV stars could be due to the fact that during the redward evolution in the HR diagram, a very massive star meets the hotter boundary of the instability strip: Mass loss increases and increases, and T_{eff} goes down until a new stable stage is reached at the low-temperature side of the instability strip. The lower g_{rad} does not sufficiently support the extended envelope, which then collapses, after which the star again settles to the high T_{eff} equilibrium stage. The details and modeling of this mechanism are still to be made.

Both models (1) and (2) are not necessarily contradictory. More probably they are complementary, since turbulent pressure effects are expected to work on the cool side of the HR diagram, while mass loss instability may be operating on the blue side.

INITIAL MASSES BETWEEN 60 $M_\odot$ AND 25 $M_\odot$ In this range, mass loss on and near the main sequence is not high enough to remove all the outer envelope, and thus the star rapidly becomes a red supergiant because the intermediate convective zone is small or absent [effect (*c*)]. The star spends part of the He-burning phase as a red supergiant, where it can expect a lifetime longer than that calculated from constant-mass models. In this mass range, the high stellar winds in the red supergiant stage progressively remove the outer envelope, and the star then evolves to the blue due to effect (*b*) above (60, 162, 163). It is worth emphasizing, however, that whether or not this will actually occur is entirely determined by the competition between the time scale of mass loss (rate) and the nuclear-burning time scale. With insufficient mass loss, a star may not be able to leave the red supergiant region. If a blue loop occurs, a star may then spend part of the He phase as a blue supergiant. It is interesting to note that such a blue supergiant could be differentiated from supergiants on their first crossing by their pulsation properties (154) and surface abundances. If the mass loss is high enough, the star may lose all the envelope and become a good candidate for the WR stage (60, 162, 163). This will likely occur in the mass range 40–60 $M_\odot$. In this range of mass we face the complex situation that mass loss on or near the main sequence favors the formation of red

supergiants, whereas heavy mass loss in the red may shorten the lifetime of red supergiants, since the star turns either into a blue supergiant and/or a WR star.

INITIAL MASSES BELOW 25 $M_\odot$ Below about 25 $M_\odot$ the mass loss in the blue or the red is never large enough to remove the outer layers and to produce a definite blueward motion. After the main sequence the star may either become a blue supergiant and later on a red supergiant, or it may first become a red supergiant and then undergo a blue loop during which the Cepheid instability strip may be crossed on an appreciable time scale. Later, the star becomes a red supergiant again. The reasons for which a star will follow one or the other of the two schemes have been already amply discussed. However, below the limit of about 20 $M_\odot$, the red-blue-red scheme is always followed by stars of any initial mass. It is worth noting, however, that in all cases the blue extension of the loop is significantly reduced by mass loss (27, 142, 163). In case of heavy mass loss, the loops may be entirely suppressed. On the whole, we have three major schemes of evolutionary sequences, as schematized below:

For $M > 60\ M_\odot$ Always Blue
O star–Of–BSG and LBV–WN–WC–(WO)–SN

For $25\ M_\odot < M < 60\ M_\odot$ Blue–Red–Blue
O star–BSG–YSG and RSG–WN–(WC)–SN: High $\dot{M}$
SN : Low $\dot{M}$

For $M < 25\ M_\odot$ Blue–Red
O star–(BSG)–RSG–YSG and Cepheid–RSG–SN

where the abbreviations are as follows: BSG, blue supergiant; YSG, yellow supergiant; RSG, red supergiant; LBV, luminous blue variables; WN, Wolf-Rayet star of the nitrogen sequence; WC, Wolf-Rayet star of the carbon sequence; WO, Wolf-Rayet star of the oxygen sequence; SN, supernova.

In view of the forthcoming discussion, it is worth commenting on the growth of the He core during the He phase. Two alternatives exist: either the core remains substantially smaller than in the classical case or it grows to a mass comparable to that of constant-mass models. The former case is typical of models calculated with the temperature criterion in the intermediate convective zone (if present) and low mass loss rates during the core H-burning phase. In such a case, the H-burning shell is topped by a fully convective zone that prevents the shell from migrating outwards and thus keeps the He core small (60). High mass loss rates and/or the adoption of the density criterion make the intermediate convective layer very small

(or even nonexistent). The H-burning shell cannot therefore undergo any significant replenishment, and thus it migrates outward, which increases the mass of the He core (164). The real mass size of the He core reached by a star at the end of the He phase is particularly important in relation to the efficiency of final nucleosynthetic enrichment (16, 55, 167).

4.3 *Effects of Mass Loss on the Advanced Stages*

After the He phase, the evolutionary time scales are so short that further mass loss (if it proceeds at current rates) is insignificant. Core contraction should lead to core collapse at essentially a constant total mass. Thus the effects of mass loss on further evolution are those already present at the end of the He-burning phase. In contrast with the huge effects of mass loss on evolutionary tracks, mass loss influences very little the course of central evolution up to the advanced stages (36, 60, 161, 163, 172). The physical reason for this rests on the fact that the mass of the He-C-O core at the end of the He phase is almost independent of mass loss for a large range of mass loss rates. Thus, constant-mass and variable-mass evolution are seen to follow the same path in the T_c vs. ρ_c diagram (Figure 4). Moreover, a comparison of the internal distribution of chemical elements and the run of temperature and density shows identical results in models with or without mass loss. Thus, in a simplified but meaningful description, a "red giant" can be considered a white dwarf surrounded by an extended envelope, much as a "red supergiant" can be considered a WR star surrounded by a very large envelope. In the case of a white dwarf, the He-C-O core is degenerate and smaller than the Chandrasekhar mass, whereas the WR star is not degenerate and has a large mass. Even for moderate reduction of the He-C-O core in the WR stars of type WC (see Section 7.1), the departures from the standard path in the T_c vs. ρ_c diagram are very small (172). Thus most (but not necessarily all) mass-losing OB stars are likely to still undergo a phase of core collapse. An essential effect of mass loss, however, is that above an initial mass of about 30–40 $M_\odot$, the supernova precursor will be a hot blue star (WR star), while below this limit the supernova precursor is expected to be a red supergiant.

Supernovae from WR precursors are expected to present the following characteristics (172): (*a*) a lack of hydrogen; (*b*) the presence of two winds—a slower one from the WR star and a fast one from the supernova (cf. 204 for Cas A); (*c*) the slow wind is likely to contain elements typical of WR stars, as indicated in Figure 5 (enhanced ^{14}N, ^{17}O and depleted ^{12}C for WN progenitors, enhanced ^{12}C, ^{16}O, ^{22}Ne and depleted ^{13}C and ^{14}N for WC progenitors); (*d*) reduced thermal and optical effects (37, 45); (*e*) the fast material must be enriched by elements of the "onion-skin" stellar model (48, 134). Cas A appears as the prototype of this faint supernova

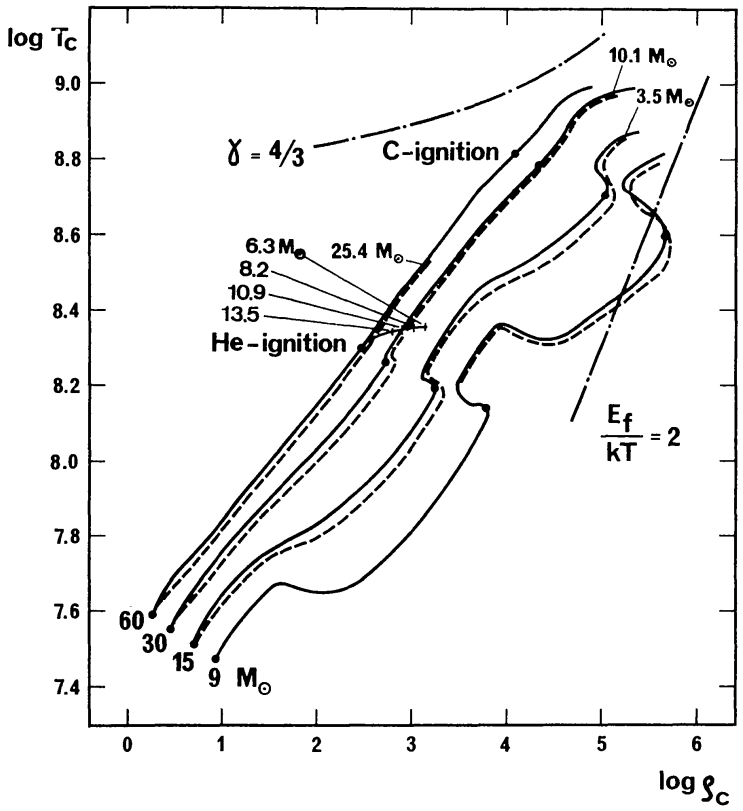

Figure 4 Evolution of models of initial mass 9, 15, 30 and 60 $M_\odot$ in the log T_c vs. log ρ_c plane (central temperatures vs. densities). The continuous lines are the tracks for constant-mass evolution, and the broken lines are those for heavy mass loss (cf. 163, case C). For the 60-$M_\odot$ star, a track corresponding to a higher mass loss rate is shown together with the current values of the remaining mass. The lines where the ratio γ of specific heats at constant pressure and constant volume is equal to 4/3, and where the ratio of Fermi energy to the thermal energy of the electrons is equal to 2, are also indicated (cf. 172).

precursor (45–47). Recent studies of the abundances in Cas A (125) may put further constraints on the nature of its precursor. Finally, we also note that the fate of the nearly fully evaporating stars—a phenomenon that is marginally possible in view of the observed mass loss rates of WR stars—has not yet been investigated.

5. THE EFFECTS OF MASS LOSS ON THE HR DIAGRAM OF LUMINOUS STARS

In this section we discuss the HR diagram (Figure 1) for luminous stars within 2 to 3 kpc of the Sun [listed in the catalogue by Humphreys & McElroy (116)] in light of stellar models with mass loss by stellar wind.

Features of the diagram relevant to this aim are the following: the group of intrinsically very bright hot stars (O and early-B types) with luminosity

in the range $-10 > M_{bol} > -12$; the lack of stars of later spectral type at these luminosities and a steady decline of luminosity with cooling effective temperature (luminosity limit for OB stars) for the earliest-type stars; the upper luminosity limit at $M_{bol} = -9.5$ extending from B3 to M supergiants; the lack of very bright M supergiants; and the peculiar location of WR and LBV stars.

We begin with a few comments of general nature and then concentrate on a result of stellar counts that has motivated most of the recent theoretical work in this area. First, the luminosity limit for OB stars depends on the relationships between spectral types (Sp), effective temperatures (T_{eff}), and bolometric corrections (BC). The HR diagram of Figure 1 rests on the so-called "quasi-hot scale of T_{eff}." On the one hand, this scale has received widespread consensus, but on the other it increases the slope of the limit to the distribution of O stars in the HR diagram. Other scales of T_{eff} are known to exist that associate a cooler T_{eff} to a given spectral type, and these make the above trend less pronounced. Second, the question may arise whether the T_{eff} resulting from evolutionary computations is comparable to the T_{eff} given by observations. Optically thick stellar winds may in fact produce a photosphere in the flow itself, which thus indicates a T_{eff} that may be significantly cooler than the one derived from hydrostatic atmospheres (26, 153). Finally, the source catalogue likely suffers from a certain degree of incompleteness that is difficult to assess. This may be particularly severe for the earliest- and latest-type stars, for which the bolometric corrections are the greatest.

Stellar counts per spectral type indicate that the star frequency distribution seems not to mimic the distribution of relative lifetimes one would expect from theoretical models. It appears that there is a deficiency of bright O-type stars near the zero-age main sequence, and that this deficiency seems to occur among O-type stars brighter than $M_{bol} = -8$ (or, equivalently, more massive than about 30–40 $M_{\odot}$). Does this indicate that stellar models are in error or that the majority of O-type stars are already evolved? We touch upon this point later on (see Section 10). In addition, stellar counts by Meylan & Maeder (187) and Bertelli et al. (26) suggest that a deficiency of core H-burning stars (main sequence band) with respect to the evolved stars is likely to exist also in other luminosity intervals. In fact, while about 10–20% of the total lifetime of a star is spent outside the main sequence band, the observations indicate that some 40% of the stars fall outside this region. To illustrate this point, we present in Table 3 stellar counts performed in a suitable luminosity range and at a suitable distance from the Sun in order to minimize effects arising from incompleteness and suspected paucity of bright O-type stars. To this aim, all stars of the Humphreys & McElroy (116) catalogue in the luminosity

Table 3 Number counts based on the Humphreys & McElroy (116) catalogue for stars with luminosity in the range $-7 > M_{bol} > -9$ and within 2.5 kpc of the Sun[a]

Constant-mass evolution: the main sequence band extends up to Sp: O9.5								
Spectral range	O	B	A	F	G	K	M	WR
Star numbers	270	380	14	7	5	2	45	20
Percentages	37.4	51.1	1.9	0.9	0.7	0.3	6.1	2.7
Evolution with mass loss: the main sequence band extends up to Sp: B0.5								
Spectral range	O–B0.5	B1–9	A	F	G	K	M	WR
Star numbers	503	147	14	7	5	2	45	20
Percentages	67.7	19.8	1.9	0.9	0.7	0.3	6.1	2.7
Evolution with mass loss and convective overshooting: the main sequence band extends up to Sp: B1								
Spectral range	O–B1	B1.5–9	A	F	G	K	M	WR
Star numbers	572	78	14	7	5	2	45	20
Percentages	77.0	10.5	1.9	0.9	0.7	0.3	6.1	2.7

[a] The total number of stars is 743. The WR stars of van der Hucht et al. (111) are added to the sample (see text).

interval $-7 > M_{bol} > -9$ and within 2.5 kpc of the Sun are used. These are complemented with the WR stars of the van der Hucht et al. (111) list falling within the same luminosity and distance ranges, since according to current evolutionary schemes (cf. Section 8.2), WR stars are the descendants of luminous OB stars. However, the luminosity of WR stars has to be taken as merely indicative owing to the well-known uncertainty in the determination of this quantity. The different groupings of spectral types given in Table 3 are meant to indicate the maximum extension of the main sequence band for models evolved at constant mass, with mass loss, and with mass loss and convective overshooting (cf. Section 6), respectively. The discrepancies are evident. It appears as if either the star counts are severely biased by incompleteness and/or selection effects or else the theoretical main sequence band has to extend up to at least spectral type A0.

5.1 *The Upper Luminosity Limit of OB Stars*

The dependence of the low-T_{eff} edge of the main sequence band on the mass loss rate [originally pointed out by Chiosi et al. (60) and since then taken as a constraint on the mean mass loss rate during the H phase (59, 138, 160)] can perhaps explain the upper boundary to the luminosity of OB stars and its steady decline with cooling T_{eff}. A comparison of model

location with the observed distribution of stars seems to indicate that rates slightly higher than those adopted to construct the HR diagram of Figure 3 are about right. However, two assumptions are implicit in the above conclusion: (*a*) the rate of mass loss depends on the luminosity alone, and (*b*) all stars near the luminosity limit are core H-burning stars. On the other hand, when mass loss rates such as those by Andriesse (9), Chiosi (53), and Lamers (136) are adopted, the main sequence band is nearly identical to that of constant-mass models, since very little mass is lost with these rates (cf. Figure 3). We also note that under all current rates (and in particular, under those dependent on luminosity, mass, and radius), the He-burning band of most massive stars is expected to be located near the main sequence. Unless core He-burning stars appear only as WR stars (the most likely situation) and thus are easily identifiable from other stars, they will crowd the same area as less evolved objects. The observational limit is therefore due to a more complicated balance between the mass loss rates in different evolutionary phases, and thus it loses its efficacy as a constraint on the mass loss during the core H-burning phase alone. Whether this boundary can be identified with the de Jager limit has not yet been assessed. Finally, stochastic effects in the initial mass function for massive stars may also be present (56), which thus makes the interpretation of the observed luminosity limit even more intricate.

5.2 *Lack of Very Bright Red Supergiants*

The lack of very bright red supergiants at $M_{\rm bol} < -9.5$ can be easily attributed to mass loss. This possibility was first explored by Chiosi et al. (60) and Humphreys & Davidson (115). The mass limit for a star being able to definitely avoid the red supergiant phase depends on the amount of mass lost in the previous phases. Current mass loss rates give an estimated limit of 50–60 $M_{\odot}$.

5.3 *Blue-Yellow-Red Supergiants With Luminosity* $-7 > M_{\rm bol} > -9$

The main sequence band of models with mass loss extends to cooler $T_{\rm eff}$, and the core He-burning band to a wider range of $T_{\rm eff}$, than do the classical models. One may argue, therefore, that a suitable tuning up of the mass loss rates for both phases may perhaps yield the desired spread of models across the blue, yellow, and red supergiant area. Even if the goal can be achieved as far as model location is concerned, it still can be easily seen that the relative percentages of blue, yellow, and red stars as compared with those of the main sequence objects cannot be accounted for by current models, even with mass loss (cf. the data of Table 3). If uncertainties in the chemical composition and observational data are allowed for, it still

seems that theory and observations are in conflict. This means that either the observational data for early-type stars (mostly OB) are still badly incomplete even in this luminosity interval, or else some deep revision of the whole physics involved in model construction is needed. Among other possibilities, the inclusion of convective overshooting in stellar interiors produces the most interesting and novel results for both massive and intermediate-mass stars (27, 32, 81, 82, 174). The effect of convective overshooting on massive stars with mass loss by stellar wind taken into account is discussed in Section 6.

5.4 *Effects of Metallicity on the Mass Loss Rates*

Among the many parameters that may affect the evolution of massive stars with mass loss, metallicity may play an important role. We distinguish two dominant effects that are deeply related, namely (*a*) effects of metallicity (chemical composition in general) on model structure, and (*b*) effects of metallicity on mass loss rates. Furthermore, we must distinguish between variations in the mass loss rates produced by metallicity in the domain of blue and red stars, since their impact on model structure would not be the same.

EFFECTS OF METALLICITY ON MODEL STRUCTURE The response of stellar models to variations in chemical composition has long been known. An increase in metallicity (Z) would yield redder models, with the main sequence, the core He-burning band, and the Hayashi line all shifted to lower $T_{\rm eff}$. Loops in the HR diagram, if they occur, are also confined to lower $T_{\rm eff}$. Since the main opacity source in O-type stars is electron scattering, the effects of changing metallicity are generally small in main sequence stars. An increase in the hydrogen content (X) will lower the luminosity without changing the effective temperature of relevant stages. The lifetimes of all nuclear stages increase at increasing X and/or Z. The ratio of blue to red core He-burning lifetimes also increases at increasing X and/or Z. Details on the evolution of a typical massive star (20 $M_{\odot}$) for various combinations of X and Z can be found in Barbaro et al. (20). These general trends still remain when mass loss is taken into account.

METALLICITY AND MASS LOSS RATES OF EARLY-TYPE STARS The radiation pressure theory of mass loss predicts that the rate for early-type stars will be proportional to the metal content (4). Although the effect of a lower metallicity on the mass loss rates may be somewhat masked by the opposite effect of metallicity on the luminosity, we still customarily expect the mass loss rates to be lower in stars of lower metal content. The observational confirmation of this prediction is uncertain and difficult to obtain. Observations of early-type stars at various galactocentric distances, which pre-

sumably possess different metal contents, are not sufficiently accurate to provide clearcut evidence of a systematic decrease in the mass loss rate with increasing distance from the galactic center [and hence with decreasing Z (95)]. Similar studies of early-type stars in the Magellanic Clouds, where the metallicity is lower than in the solar vicinity, have perhaps indicated that stellar winds are weaker compared with their galactic counterparts (34, 118). Garmany & Conti (96) estimate that for O-type stars of luminosity classes III and V, the terminal velocities in the Large Magellanic Cloud (LMC) are about 600 km s^{-1} lower than in the Galaxy. Terminal velocities in the Small Magellanic Cloud (SMC) are about 1000 km s^{-1} lower than in galactic stars. However, the conclusion that the mass loss rates are also lower than in galactic stars is very uncertain, and there is no confirmed difference in the mass loss rate for galactic and Magellanic Cloud stars.

METALLICITY AND MASS LOSS RATES IN LATE-TYPE STARS In this domain, both theories and observations of mass loss are so uncertain that nothing can be said about the dependence of mass loss rates on chemical composition (and on Z in particular). For red supergiants, Kwok (132) has suggested an increase of the rate with metallicity, although the dependence might be weaker than for early-type stars, if any exists at all.

The safest conclusion in this respect is to say that neither theory nor data are sophisticated enough to address the question of the dependence of mass loss rates on the chemical composition. Despite the above uncertainties, the notion that the mass loss rates should be lower for lower metal content has received some attention, and models to represent the evolution of massive stars of lower metallicity have been calculated (105, 207). The global results do not differ very much from those with normal metallicity, and as expected, they are quite similar to those for constant-mass stars of the same metal content. Nevertheless, the dependence of the mass loss rates on the initial metallicity has been often invoked to interpret the observed gradients in WR, blue, and red supergiant stars across the galactic disk (188, and references quoted therein) and to explain the variation of the relative frequency of single versus binary WR stars, together with their relative frequency per spectral subtype passing from the Galaxy to the LMC and SMC (262).

6. EVOLUTION WITH CONVECTIVE OVERSHOOTING AND MASS LOSS

From the stellar counts by Meylan & Maeder (187) and Bertelli et al. (26), the conviction arose that the main sequence band of bright stars confined

in the luminosity range $-7 > M_{bol} > -9$ (cf. Section 5 and the data of Table 3) should extend up to the spectral type A0. Such a demand suggested that an important ingredient of model structure was still neglected in evolutionary computations.

In the classical computations of stellar structure, the boundary of the convective core is determined by the Schwarzschild condition ($\nabla_{TR} = \nabla_{TA}$). It can be shown that this is equivalent to saying that the acceleration imparted by the buoyancy force to convective elements vanishes at the layer where the above condition is satisfied. However, the velocity of convective elements is not zero, which implies that they penetrate (overshoot) into the formally stable radiative zones and thus increase the mass of the convective core. It was long thought that overshooting was negligibly small (219), but more recently some workers have pointed out that the scale length of this phenomenon may be significant (26, 27, 32, 62, 63, 81–83, 157, 158, 174, 183, 215, 227, 250). Convective overshooting is customarily formulated with the aid of the mixing length theory of convection, and it uses the mean free path of convective elements expressed by $l = \Lambda H_p$, where H_p is the pressure scale height at the edge of the classical core, as a free parameter (Λ).

A completely different formulation is given by Roxburgh (215), whose model apparently contains no free parameters. However, most of the computations so far are based on the first type of formulation, whereas Roxburgh's condition has been adopted to this point only by Doom (83). Even if there are uncertainties on the theoretical side, the numerical results show that the two formulations give equivalent results for Λ in the range 1 to 2.

The main results of model computations with convective overshooting and mass loss by stellar wind taken into account can be summarized as follows:

1. The mass of the convective core is significantly greater than in classical models. As a consequence, semiconvection and/or full intermediate convection never develop. This holds true for both constant-mass and mass-losing models and thus definitely rules out the well-known uncertainty of semiconvective instability.
2. Stars are expected to evolve toward higher luminosity than in classical models, independent of whether or not mass loss is included.
3. Convective overshooting increases the lifetime of the core H-burning phase, since more fuel is available, which largely overwhelms the effect of a higher luminosity (157, 158). The increase in lifetime is by far greater than that due to mass loss alone.
4. The main sequence band at the lower mass range is much wider than

ever before under the combined effects of convective overshooting and mass loss. At higher masses, constant-mass models with overshooting would spread across the whole HR diagram, even during the H-burning phase. However, with models including convective overshooting and mass loss, the core H-burning band shrinks toward the zero-age main sequence, in a manner similar to models with very high mass loss alone. The new location of the main sequence band for masses in the range 20–60 $M_\odot$ is particularly interesting, since it may now extend up to spectral type B1 instead of O9.5 as for models with mass loss and no overshooting. The new models spend about 20% of the total core H-burning lifetime in the spectral range B0–1 (26, 32), which roughly amounts to the total core He-burning lifetime. Consequently, we expect in this spectral range (which approximately corresponds to the Hertzsprung gap of classical models) as many stars as in all other later spectral types. As shown by Bertelli et al. (26), this result may alleviate the difficulty of the many stars falling outside the main sequence band of classical models.

5. The core He-burning lifetime is not greatly affected by overshooting and is only modestly increased. The ratio of core H- to He-burning lifetimes is about 0.06. The He phase takes place partly in the red supergiant region and partly in the blue (WR candidates) for initial masses between 20 $M_\odot$ and about 50 $M_\odot$. Approximately one third of the core He-burning phase is spent by a typical 20-$M_\odot$ star as a red supergiant. On the contrary, stars more massive than about 50–60 $M_\odot$ spend the whole He phase as blue stars located on or near the zero-age main sequence. On the whole, the scenario elaborated for stars with mass loss alone still holds for those with both convective overshooting and mass loss. The details, however, are profoundly different.

The number frequencies per spectral type expected with the new models are reported in Table 3 for purposes of comparison with those derived from classic calculations. Although a fully satisfactory reproduction of the HR diagram of Figure 1 is not yet possible even for models with overshooting, theory now seems to show better agreement with observations, as can be seen by the numerical simulations of synthetic HR diagrams performed by Nasi (191).

7. NUCLEOSYNTHESIS

7.1 *Changes of Surface Abundances*

Surface abundances, which may change during evolution as the result of convective dredge-up, of mass loss, and of possible internal mixing processes, constitute a powerful test of stellar evolution. The changes of

abundances in massive stars due to mass loss and dredge-up have been calculated by Noels et al. (195), Noels & Gabriel (196), Maeder (166), and Greggio (101). The main effects are illustrated in Figure 5. At the beginning of stellar evolution, the surface abundances are the standard ones (i.e. the abundances of the parental interstellar material). Then, as a result of removal of the envelope, elements that were originally located in the convective core appear at the stellar surface and provide evidence of CNO-processed material. As the CN cycle rapidly reaches equilibrium, the C/N ratio almost abruptly changes from 4.1 to 0.03 (in mass). The O/N ratio

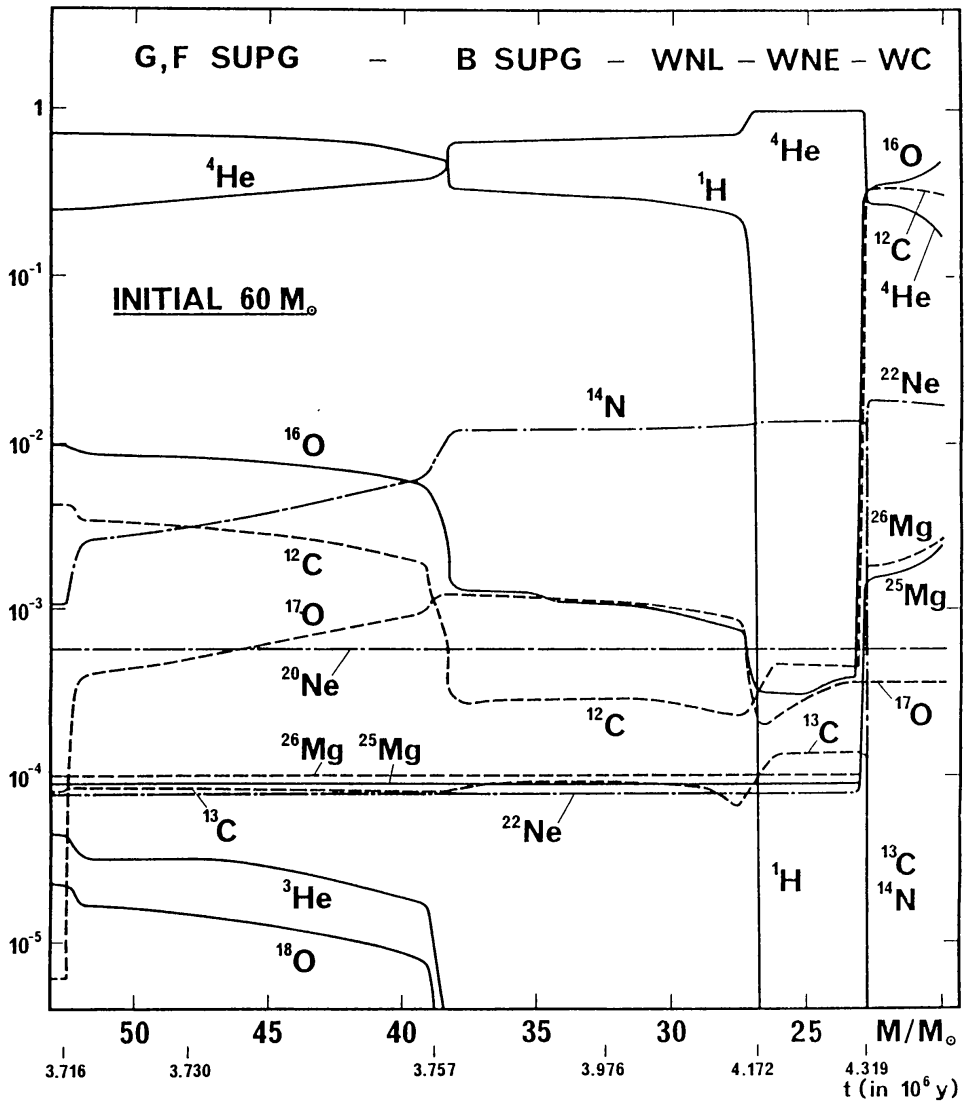

Figure 5 Changes of the surface abundances (in mass fraction) in terms of the remaining mass for the model with an initial mass of 60 $M_{\odot}$. The ages are also indicated on the lower axis. At the top of the figure, the corresponding evolutionary status is given. On the left, the original cosmic abundances of the elements are given. The surface abundances are changing as a result of convective dredge-up and mass loss (cf. 171).

slowly changes from 9.1 to less than 0.1 because the ON cycle takes a longer time to reach equilibrium. The abundance of ^{13}C is usually a factor of 3.3 below that of ^{12}C. The elements ^{3}He, ^{15}N, and ^{18}O disappear. The various plateaus in the supergiant phase are due to convective mixing in various parts of the star models. In giants and supergiants the CNO-processed material is diluted within the stellar envelope; this is not the case for WR stars, which directly exhibit the processed material at the surface.

If peeling off proceeds far enough, the products of He-burning reactions prominently manifest themselves at the stellar surface. This corresponds to the WC stage. A very large discontinuity marks the appearance of the He burning at the surface (cf. Figure 5): This is likely to correspond to the beginning of the WC stage. The physical reason for this discontinuity is that the convective core increases in mass during most of its evolution in the He-burning phase, and a chemical discontinuity is thus built at the border of the core at its largest extension. We note then a very steep disappearance of ^{13}C and ^{14}N, a very temporary peak of ^{18}O, and above all a vertiginous rise (by more than two orders of magnitude) of ^{12}C, ^{16}O, and ^{22}Ne (Figure 5). The abundances of ^{25}Mg and ^{26}Mg also rise strongly, particularly in the most massive "WC stars," where *s*-elements are enhanced as a result of neutron capture from ^{22}Ne $(\alpha, n)^{25}Mg$ reaction.

The LBV and WR stars are the best examples for changes of surface abundances. In the case of the LBV star η Carinae, Davidson et al. (76, 77) determined the abundances in some of the outer condensations surrounding the central nebula and found ratios $C/N < 0.05$ and $O/N < 0.15$–0.5 (in number). These ratios differ very much from the solar ones ($C/N = 4$, $O/N = 9$) and are in full agreement with the values obtained in the blue supergiant phase of an initial 120-$M_\odot$ star evolving with mass loss (166). These observed abundances provide a strong constraint on the long-standing problem (249) of the evolutionary status of LBV stars.

In the conspicuous case of WR stars, observations of chemical abundances have been made and analyzed by Conti et al. (71), Nugis (201), Smith & Willis (234), and Willis (267). Generally speaking, the observed abundances for WNL, WNE, WC, and WO stars are consistent with a progression in the exposition of nuclearly processed material from the CNO cycles and then from the He-burning reactions. From the point of view of surface abundances, these four groups of WR stars are distinguished (68, 267) as follows:

1. The WNL (WN6–9) stars, which still have some hydrogen at the surface and which should be produced by relatively modest peeling off of very massive stars.

2. The WNE (WN2–6) stars, which generally have H/He = 0 and which should be generated by those stars that are able to lose all their H-rich envelope.
3. The WC stars, which have no hydrogen and an extremely high C/N ratio. According to our nucleosynthetic scheme, they should correspond to the case when He-burning products are exposed at the surface during early stages of the core He-burning.
4. The WO stars, which are essentially similar to WC stars but with O enhancement (23). Whether they represent the case of extreme peeling off during core He-burning when C has become less abundant than O (late stages) is not well assessed.

The observed C/He, N/He, and C/N ratios were compared with model predictions and a general agreement was found (166), which is a strong confirmation of the advanced evolutionary stage of WR stars.

7.2 *Effects of Stellar Winds on Galactic Enrichment*

Each generation of stars contributes to the chemical enrichment of the interstellar medium (and of a galaxy as a whole) by processing new material in the stellar interiors and returning to the interstellar gas a fraction of its total initial mass containing both processed and unprocessed matter during the various stages of mass ejection (stellar winds, supernova explosion, etc.). In the following, we focus on massive stars only, which are known to be the dominant sources of helium and heavy elements. Estimates of the amounts of helium and heavy elements produced by massive stars have been made by Arnett (16), Chiosi (50), Chiosi & Caimmi (55), Chiosi & Matteucci (57), Maeder (164, 167), and Mallik (175, 176). Not all procedures used by the various authors are strictly equivalent, and thus some clarification is necessary for the correct use of theoretical yields in models of galactic enrichment.

Nucleosynthetic enrichment in massive stars has been studied by Arnett (16); in this study, pure helium stars thought to represent the central core of more massive objects were followed until the presupernova stage. The same approach has been adopted by Arnett & Thielemann (17) and Thielemann & Arnett (255) using updated nuclear reaction rates. On the other hand, Woosley & Weaver (273) and Woosley et al. (272) have calculated complete models of massive stars evolved at constant mass until the stage of supernova explosion. The nucleosynthetic data for bare core calculations [and to a lesser extent, the data for complete stellar models] were transferred to those of standard stars adopting a suitable $M(M_{He})$ relationship (initial mass versus the He core mass M_{He}). Immediately an uncertainty arises from the fact that M_{He} is not constant in the course of

evolution but rather depends on many details of model structure, such as the mass loss rates till the stage of C exhaustion in the core. It is therefore clear why different $M(M_{He})$ relations have been found by different authors, each of which is equally legitimate in light of all the uncertainties still affecting the evolution of massive stars. A second point of complexity comes from the distinction between amounts of newly processed elements ejected in the stellar wind, and thus subtracted to further nuclear processing, and those in the final supernova explosion. Most of the yields computed so far neglect the effects of stellar winds, which on the contrary may play a dominant role, and consider only the effects of supernova explosion. Maeder (164) and Abbott (6) first included the contribution of winds to the yields of several important elements. To illustrate this point and make clear how important the contribution of the stellar wind is as compared with that of the supernova explosion, we show in Figure 6 the fractional

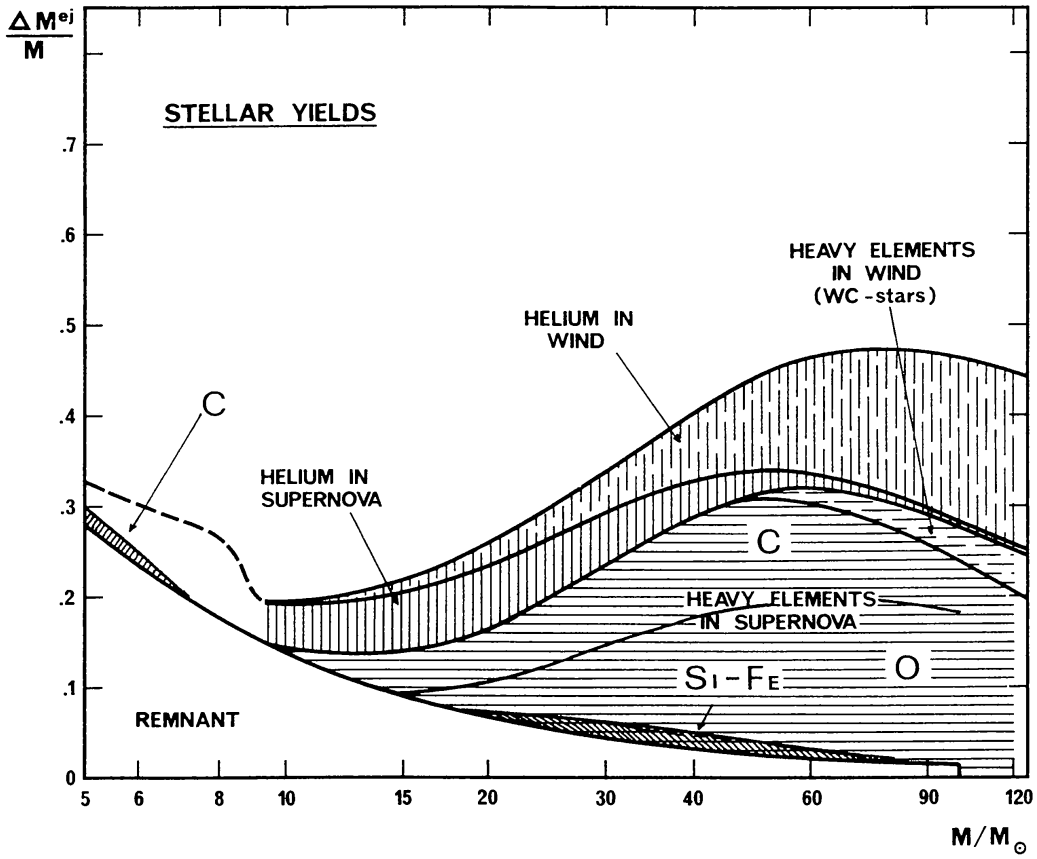

Figure 6 Mass fraction of new helium and new heavy elements ejected as a function of the initial stellar mass. Contributions from stellar winds of OB stars, supergiants, and WR stars are totaled and distinguished from the contribution from supernova explosions. The distribution of heavy elements in the supernova ejecta is based on the classic value for the $^{12}C(\alpha,\gamma)^{16}O$ reaction rate (see text). The contribution to ^{12}C by intermediate-mass stars is derived from Renzini & Voli (214) and is limited to their case A.

masses of several important elements (He, C, O, and Si-Fe group lumped together) ejected by massive stars in occurrence of significant mass loss (167). The separate contribution to helium and heavy elements by the stellar wind and supernova explosion are also indicated. The particular quantities shown in Figure 6 are obtained by a detailed sheet balance, and so they do not depend on a given $M(M_{He})$ relation. However, they do depend on the particular history of mass loss during core H and He phases and on details of model structure. Furthermore, the repartition between C and O shown in Figure 6 refers to nucleosynthesis data obtained with the $^{12}C(\alpha,\gamma)^{16}O$ reaction rate of Fowler et al. (89), since no sufficient calculations with the new rate of Kettner et al. (127) are available today. For helium, we clearly note the increasing importance of the wind with increasing stellar mass, whereas the amount of helium ejected in the supernova explosion becomes negligible. For heavy elements, the contribution of the wind becomes important above a mass limit that is relatively high. This contribution comes from stars in the WC stage. However, the amounts of heavy elements ejected in the supernova explosion always remain preponderant over the wind contribution. The fractional mass of stars locked forever in the 1.4-$M_\odot$ neutron-star remnant is also shown for purposes of comparison.

Weighting the stellar yields of Figure 6 by the initial mass function is now necessary to properly derive the yields per stellar generation to be used in chemical models of galaxies. The whole procedure for the correct formulation of this quantity and of the general equations of galactic evolution can be found in Tinsley (256) and Chiosi & Matteucci (57), to whom we refer for all details. The choice of an initial mass function is another source of uncertainty, since many formulations of this quantity exist (220). Detailed calculations of the global yields of several important elements for various initial mass functions and stellar nucleosynthetic input are by Chiosi & Matteucci (57), Maeder (167), and Mallik (175, 176).

It has long been suggested that the helium abundance Y is correlated to the metal abundance Z. Peimbert & Torres-Peimbert (205, 206) estimate the ratio of relative helium to metal enrichment to be $\Delta Y/\Delta Z = 3$. This ratio is, however, a matter of vivid debate. On one side, recent observational determinations for a group of dwarf irregular galaxies having the lowest metallicity seem to indicate a large scatter in Y, which somewhat invalidates the above relation (131). On the other side, the high value found by the Mexican group has so far eluded simple theoretical explanations. A thorough discussion of this issue can be found in Maeder (167) and Chiosi & Matteucci (57). In brief, while helium is predominantly produced by all stars less massive than about 30 $M_\odot$, heavy elements are predominantly produced by massive stars, with the exception of the significant production

of C and N by intermediate-mass stars (214). The ratio predicted by current models of massive stars (mass loss and no convective overshooting) and current initial mass functions is not greater than 1.3 (167). An obvious way out of this difficulty is to lower the amount of heavy elements ejected by massive stars by varying the mass limit above which core collapse at the stage of supernova explosion produces black holes. In fact, there must be a relation between the $\Delta Y/\Delta Z$ ratio and the lower mass limit M_{BH} for black hole formation (cf. 168). For M_{BH} as high as 150 $M_\odot$, the $\Delta Y/\Delta Z$ ratio is about 1.3, a value that rises up to about 3 for $M_{BH} = 20\ M_\odot$. While the theoretical value for M_{BH} is still quite uncertain, some observations of pulsars in double systems (cf. 107) and in young associations (223) suggest a value of M_{BH} as high as 50 $M_\odot$. However, a major uncertainty rests on the location of the mass cutoff between the collapsing core and the matter blown away in the supernova ejecta. A possibility of lowering the metal yield is perhaps given by the recent models for massive stars, which incorporate the new cross section of the $^{12}C(\alpha, \gamma)^{16}O$ reaction rate (127, 141). With the new rate, which runs at least three times faster than the classic one of Fowler et al. (89), the carbon-oxygen core is replaced by a core of almost pure oxygen at the end of the He phase. Whether this fact may affect core collapse, with likely formation of a black hole rather than a neutron star, in the domain of massive stars instead of very massive stars (30, 86, and references therein) is only now beginning to be investigated (271). In such a case, massive stars would produce mostly O and little amounts of Si-Fe. Such a possibility has also been advocated by Chiosi & Matteucci (57) to explain the chemical history of the galactic disk and the variations of the abundance ratios |O/H|, |C/H|, and |Fe/H|.

8. THE PUZZLING NATURE OF WR STARS

8.1 *Properties of WR Stars*

WR stars play an important role in the overall understanding of massive star evolution. In fact, they are thought to represent the descendants of massive stars via the mechanism of mass loss. WR stars, whose spectra are dominated by strong emission lines, are generally grouped into three spectral sequences: WN, WC, and WO. The spectra of WN stars exhibit transition lines of He and N ions with little evidence of C; those of WC stars predominantly show lines of He and C with little evidence of N; while the spectra of rarer WO stars are dominated by lines of oxygen. In general, WN stars show little or no evidence of hydrogen, and no hydrogen is seen in WC and WO stars. However, WN stars are commonly separated into two further groups according to whether or not they show evidence of some significant H. Broadly speaking, this separation corresponds to

that between early (WNE—little or no H) and late (WNL—some significant H) WN stars. Exceptions are known to exist in both sequences. Whether the lack (little evidence) of C in WN stars and of N in WC and WO stars reflects real underabundances of those elements, or is instead the result of unusual excitation conditions in their atmospheres, is still controversial, although the former interpretation is presently favored (267). Detailed analyses supporting the chemical anomaly hypothesis are by Nugis (200, 201), Smith (232), Smith & Willis (234), and Willis & Wilson (269), whereas arguments in favor of excitation conditions and normal abundances have been made by Underhill (257–260).

One of the most important questions relative to WR stars is whether they are all members of binary systems, or rather do some truly single objects also exist. Summarizing recent work on this subject (178–182, 194, 262), we conclude that many of the WR stars with absorption lines appear to be truly single, and that the percentage of visible close WR + OB binaries seems at most 34% (110). Taking into account WR stars with collapsed companions, van den Heuvel (106) suggested that the true percentage of binary WR stars should be higher.

Luminosities and effective temperatures of WR stars are very uncertain. What is reasonably well established is the absolute visual magnitude for a small number of stars with known distance (cf. 69). Effective temperatures derived by various authors differ greatly. Recent analyses are by Conti (65, 66, 69), van der Hucht et al. (111), Kudritzki (130), Underhill (257, 258), and Willis (266, 268). Broadly speaking, the effective temperatures are in the range 25,000–50,000 K; values as high as 10^5 K have also been proposed. It is therefore clear that the location of these stars in the HR diagram is highly uncertain, even if one may reasonably assume that they lie near the upper main sequence in the same region of the brightest O-type stars, as indicated in Figure 1. The distinct groupings for WNL (hotter and brighter) and WNE, WC, and WO stars proposed long ago by Conti (66) are adopted in Figure 1 for purposes of simplicity.

The mass of WR stars is also poorly known. Mass determinations within the usual factor of $\sin^3 i$ for the few stars in binary systems range from 10 to 50 $M_\odot$, with an average value of about 20 $M_\odot$ (179, 180). Attempts at establishing a correlation between the WR subtype and the mass ratio M_{WR}/M_{OB} gave controversial results (179, 189). According to Niemela (193), estimates of the minimum mass of binary WR stars reveal that WNLs are more massive than WNEs (38 and 7 $M_\odot$, respectively), whereas late WCs can be considered as having masses in excess of 15 $M_\odot$. No useful data exist for binary WCs of early spectral type. Single WR stars elude direct mass determinations, so that nothing can be said.

Finally, no fully satisfactory physical interpretation of the spectral

sequences in terms of the basic stellar parameters has been obtained, nor has the correlation between the various subtypes been fully understood. The evolutionary schemes we discuss below and which have already transpired from the discussion of surface abundances are almost entirely rooted on the results of evolutionary computations showing that progressive peeling off of the stars by mass loss exposes nuclear-processed material at the surface. Since nucleosynthesis events take place in stellar interiors in a well-established temporal sequence, a sequential ordering of WR types follows.

8.2 *The Formation of WR Stars*

The first point to examine is the initial mass of stars leading to the formation of WR stars. From studies of WR frequency, Smith (232) suggests that WR stars originate from stars initially more massive than 25 $M_\odot$ and Firmani (88) gives an estimate of 20 $M_\odot$. Considerations on evolution with mass loss indicate a limit of 20–30 $M_\odot$ (cf. 54, 163). Conti et al. (71), based on a study of the galactic distribution of WR stars, conclude that the bulk of WR stars descend from stars initially more massive than 40 $M_\odot$. This claim is supported by Schild & Maeder (222), who note, however (on the basis of WR stars in young associations), that some may originate from masses as low as 20 $M_\odot$. A similar conclusion was reached by Bertelli & Chiosi (29) and Bertelli et al. (26). The same limit is supported by de Loore's (149) study of binary evolution. Humphreys et al. (117) found a limit of 30 $M_\odot$; they also pointed out that 80% of the WR stars had initial masses greater than 50 $M_\odot$.

Several complementary mechanisms and evolutionary sequences related to the formation of WR stars have been proposed. Their relative importance, however, is not known.

1. *Through O, Of stars* This is the scenario proposed long ago by Conti (64) that, as a result of stellar winds, leads O and Of stars directly to WN7–9, WN, and WC. Quantitative models corresponding to this scenario have been calculated by Chiosi et al. (59, 60), Dearborn et al. (79), de Loore et al. (152), Maeder (160), and Noels & Gabriel (196). This scenario is likely to hold for stars initially more massive than about 80–100 $M_\odot$ and may change an O-type star into a WNL object even during the core H-burning phase.

2. *Through the O, Of, LBV stage* With the observed mass loss rates, standard models appear to be able to form WR stars with the above Conti scenario only for initial masses greater than 80–100 $M_\odot$ (the difference being due to whether or not convective overshooting is taken into account). Thus, the star follows the general scheme described in Section 4.2 for stars

initially more massive than 60 $M_\odot$. The removal of the envelope in the LBV stage leads to the formation of WR stars (166); these stars are most likely WN7–9 initially, since these WN types occur in the youngest associations (232, 233).

3. *Through the red supergiant stage* There is no LBV stage for initial masses below 60 $M_\odot$, and thus the star becomes a red supergiant, as discussed in Section 4.2. Mass loss in this stage may then lead to the WR formation after a temporary blue supergiant phase (60). The quantitative models show the following features (cf. 163): Firstly, the minimum luminosity for the formation of WR stars decreases considerably with increasing mass loss. Secondly, the fraction of the He-burning phase spent in the WR stage increases with the luminosity and the mass loss rates in the previous stages. These two facts make the frequency of WR stars very sensitive to the mass loss rates in the previous stages. The scenario through the red supergiant phase may apply to stars with initial masses above 20 $M_\odot$ (primarily in the initial-mass range of 40–60 $M_\odot$; see 117).

4. *Through mixing* Any efficient mixing process would also favor the formation of WR stars, since nuclearly processed materials are driven to the stellar surface. Moreover, mixing reduces the internal density contrast, thus favoring instabilities (see below). A likely mechanism is turbulent diffusion induced by differential rotation (165).

5. *Through binary evolution* The production of WR stars by mass transfer in binaries has been reviewed by de Loore (146, 147, 149). Various cases of mass transfer occurring at different evolutionary stages have been classified by Kippenhahn & Weigert (128). A particularly noticeable case is that of massive close binary evolution leading to an X-ray source (cf. 108, 146, 149, 150). Mass is not only exchanged between the components but also lost from the system. Vanbeveren & de Loore (263) and de Loore (147) estimated that between 50 and 75% of the matter leaves the system, carrying away some 50% of the angular momentum.

The true importance of mass transfer in WR star formation is difficult to estimate. Even if the observed fraction of known binaries in the solar neighborhood is 34% (110), this fraction does not necessarily represent the contribution of binary mass transfer to WR star formation. On the one hand, this ratio may still suffer from incompleteness; on the other, a WR star in a binary system may also owe its existence to stellar wind. From an analysis of the orbital separations and eccentricities, Massey (179, 180) finds that only the most massive O + O systems evolve to WR + O systems, and that mass transfer may not even be important in these cases. Useful information may come from the study of the relative frequency of binary WR stars at different galactic locations. Hidayat et al. (109) found

that the relative frequency of WR binaries increases with galactocentric distance and is even greater in the Large and Small Magellanic Clouds (19, 33). This fact, together with the result that the number ratio WC/WN is larger toward the galactic center (110), suggests that the relative importance of the various channels for forming WR stars changes with galactic location (163, 165), probably as a result of differences in metallicity and perhaps in initial mass function.

8.3 *Physical Properties of WR Models*

The WR models appear to obey a rather thin mass-luminosity relation ($\log L/L_\odot = 3.8 + \log M/M_\odot$; see 166). For a given mass, this relation is 1.5 to 2.5 magnitudes brighter than the initial mass-luminosity relation. The physical reason for this relation is that WR models are nearly homologous He-C-O cores. For the time being, no experimental confirmation of this relation has been achieved. The vibrational stability of helium stars has been tested for a long time (31, 197, 198, 251). He stars more massive than 16 $M_\odot$ are found unstable. However, WR models are not identical to pure He stars; H-poor envelopes exist in WNL stars, and gradients in He, C, and O may be present in WR stars. In tests of vibrational instability throughout the evolution of very massive stars, the WR stage—as defined by surface abundances—was found to correspond closely to a stage characterized by vibrational instability (170). Entry into the unstable regime occurs when the surface ratio H/He is equal to 0.3, in agreement with former models of helium stars with a thin hydrogen-poor envelope (229). The WR models remain unstable throughout the WR phase, with central nuclear energizing largely overcoming the radiative damping in the envelope. In models with relatively lower mass loss rates, the instability phase appears to be concentrated in models near the minimum of the ratio $\rho_c/\bar{\rho}$ of central to average density (196). Nonradial instabilities have also been found for high harmonics of the $g+$ spectrum (129). A central question remains as to whether the excessive mass loss rates of WR stars (24) can be accounted for by mechanical energy transferred from pulsations.

The expected lifetimes of WR stars lie in the range 3–8 $\times$ 10^5 yr (51, 52, 54, 172; see also Table 2), which correspond to fractions of about 0.1–0.3 of the main sequence lifetimes. The lower limit could raise some problems, because Conti et al. (71) found a number ratio of WR/O stars of 0.36 ± 0.15; this ratio refers to stars closer than 2.5 kpc and with an initial mass larger than 40 $M_\odot$. Convective overshooting appears to decrease the ratio t_{He}/t_H of helium to hydrogen lifetimes; a value of 0.06 was found by Bertelli et al. (26). However, such a ratio depends on the relative increase due to overshooting of the convective cores in the H- and He-burning phases. In such a case the discrepancy still exists, and this could be a sign

that a different way of looking at this problem is needed (i.e. the number of O-type stars could be incomplete with respect to the number of WR stars).

9. GALACTIC DISTRIBUTION OF O, BLUE AND RED SUPERGIANT, AND WR STARS

Star counts in different regions of the galactic disk seem to indicate systematic gradients in surface densities of main sequence (O-type), blue supergiant (B–A type), yellow supergiant (F–G type), red supergiant (M type), and finally WR stars. Although star counts in the galactic disk may be hampered by many observational uncertainties (distances, reddening, completeness, etc.), the above trends have been often taken as indicating variations in the evolutionary history of a massive star as a function of the galactocentric distance, or in other words as a function of the ambient chemical composition (metallicity). The metal content, in fact, is known to decrease outward (cf. 186 for an updated review of this subject). Meylan & Maeder (188) derived the gradients in surface densities for the five classes of stars listed above. These are shown in Figure 7, where the star samples

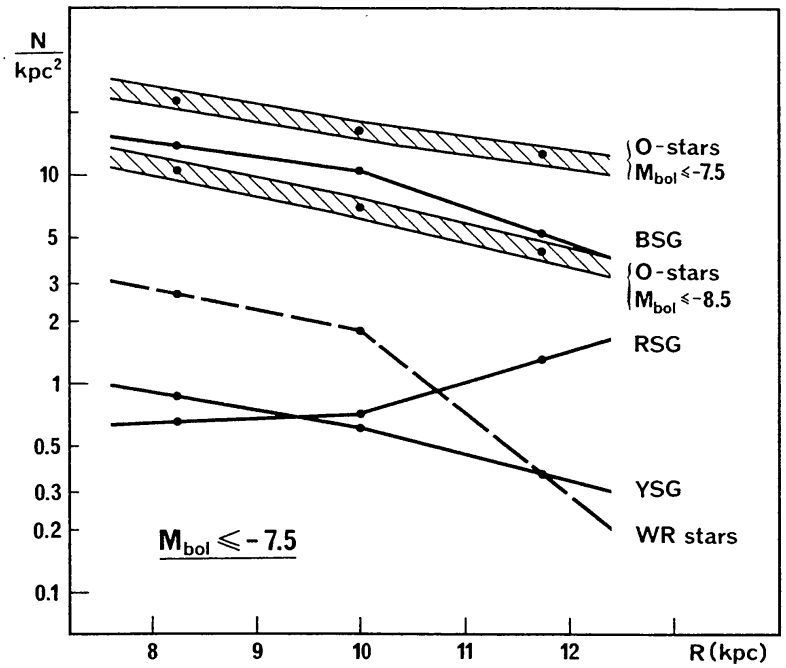

Figure 7 Surface density projected onto the galactic plane of various kinds of massive stars as a function of the galactocentric distance. Stars brighter than $M_{bol} = -7.5$ are taken here; for O stars, two different lower magnitude limits are considered, one at $M_{bol} = -7.5$ and another at $M_{bol} = -8.5$. BSG, RSG, and YSG refer to blue, red, and yellow supergiants, respectively.

have been limited to objects brighter than $M_{bol} = -7.5$ to alleviate the problem of incompleteness at lower luminosities. With the available data, it appears that the ratio $N(RSG)/N(WR)$ (number of red supergiants to WR stars) strongly decreases toward the galactic center, whereas the ratio $[N(RSG)+N(WR)]/N(BSG)$ (sum of number of red supergiants and WR stars to blue supergiants) remains virtually constant. The gradient in O-type stars increases toward the galactic center; the gradients in red supergiants and WR stars seem inversely correlated; and the gradient in WR stars (as compared with that in O-type stars), though similar, gets steeper moving outward. The existence of gradients in the ratio of blue to red supergiants, in the ratio of WR to red stars, and in the ratio $[N(BSG)+N(WR)]/N(RSG)$ has been questioned by Freedman (90) in her study of M33. However, Freedman's analysis is not conclusive, as it does not allow fine indications. Maeder et al. (173) and Meylan & Maeder (188) attributed the inverse correlation between WR and RSG stars to be a strong effect of metallicity on the formation of WR stars through the red supergiant channel. When the metallicity is high, the mass loss rate in the red is also high, and thus the formation of WR stars is facilitated. This idea was criticized by Bertelli & Chiosi (28, 29) and Garmany et al. (94), who suggested that the gradient in WR stars simply reflects the gradient in O-type stars (cf. Figure 7). However, since the gradient in WR stars is steeper than the gradient in O stars (cf. 72), and the gradient in red supergiants is of opposite sign, the gradient in WR stars cannot just reflect that in O stars (and consequently, of the initial mass function); instead, it must also reflect a variation in one of the agents by which WR stars are formed (likely a variation in the mass loss rate). The crucial aspect of such an interpretation is the very weak evidence for a dependence of the mass loss rate on the ambient metallicity (cf. Section 5.4) and the uncertainty in the minimum mass for forming WR stars. If the minimum mass is above 50–60 $M_\odot$ (cf. Section 8), then the red supergiant channel is almost ineffective, since most red supergiants seem to have evolved from stars of lower mass. This situation is even more complicated if we consider the distribution of WR subtypes across the galactic plane. In fact, Firmani (88) has pointed out that WNE stars have a distribution across the galactic plane different from all other WN types. Similar behavior is found for WC6 stars, whose distribution is different from all other WC types. Finally, the distributions of WNL and WC stars tend to concentrate toward the galactic center. The different spatial distributions between WNEs and WNLs and between WNEs and WCs perhaps suggest that WNLs are not the progenitors of WNEs and that WNEs are not the progenitors of WCs. Although the statistics backing Firmani's (88) discussion are quite poor, we still feel that this point deserves great consideration and further

discussion. It seems that WNL stars evolve directly into WC stars and thus miss the WNE stage. A possible explanation for this has been advanced by Chiosi (54) in terms of the stability properties of WR stars. He argues that the (massive) WNL stars become highly vibrationally unstable when entering the WNE stage. The instability, either by mixing or by removing the He + CNO layers (which are the signature of the WNE stage), would suppress the WNE stage and immediately reveal the products of He burning (WC stage). The instability is likely to occur in the most massive stars, since a minimum mass is required for vibrational instability to set in. The WNE phase would survive only in those stars that are able to reach this configuration with mass below the stability limit. The future developments in the number statistics of WR subtypes in clusters and associations could set constraints on the duration of the corresponding evolutionary phases.

10. OPEN PROBLEMS AND CONCLUSIONS

Compared with models with constant-mass evolution, the models with mass loss have led to substantial progress in our understanding of massive stars. The genetic connections between massive stars have been clarified, as has the role of these stars in the nucleosynthetic enrichment. Other topics that have been discussed are the consequences of mass loss on the latest evolutionary stages, and the possible effects of differences in mass loss rates on the galactic distribution of massive stars. Nevertheless, while there appears to be reasonably good agreement between the results of model calculations (with mass loss and convective overshooting) and relevant observations, difficulties still remain when a detailed comparison is performed. There are several problems that demand further clarification:

1. Completeness of the star catalogues used to compare theory with observations.
2. The effects of binary stars on the evolutionary scenarios we have been discussing so far only for single stars (i.e. how their inclusion would alter the statistics).
3. The input physics of model construction [nuclear reaction rates, opacity, diffusion, mixing processes (convective overshooting, turbulent diffusion, semiconvection), treatment of the outer layers and nonhydrostatic atmospheres, etc.] or, in other words, how close to real stars are the current stellar models.

However, there are several points of major uncertainty. For example, it has been already noted that the Humphreys & McElroy catalogue of luminous galactic stars is certainly affected by some degree of incom-

pleteness that is difficult to establish. This main source of data is likely fairly complete down to $M_{bol} = -8$ and within 2.5 kpc of the Sun. We insist on this point, because such a composite HR diagram is a good source and may provide us enough data to allow tests of theoretical models of massive stars. Furthermore, owing to its composite nature, this HR diagram encompasses all ages relative to the most massive objects, so that the past history of star formation plays only a marginal role. Doom et al. (84) argued for time-dependent star formation in OB associations (in the sense that lower mass stars form first) in order to defend current models of massive stars; however, while such star formation may hold for individual associations (thus making the interpretation of observational data even more complicated), it does not apply to such a composite HR diagram. The major uncertainty with this HR diagram is related to the suspected paucity of O-type stars brighter than $M_{bol} = -8$ near the zero-age main sequence, which perhaps suggests that a significant fraction of potential O-type stars are not detected as such because they are still embedded in their parental cloud. This may likely happen when the evolutionary time scale (nuclear) is comparable to the time scale required to dissolve the parental cloud (12, 94, 261). The fraction of these invisible O-type stars is very uncertain. An estimate by Metzger (185) suggests about 20%. Since this corresponds to the mass range in which the majority of WR stars form (cf. Section 8), the problem of the observed high $N(\mathrm{WR})/N(\mathrm{O})$ ratio could possibly be solved without invoking other modifications to current stellar models. Conversely, the theoretical zero-age main sequence may be too blue as compared with the bulk of very luminous O-type stars. This would imply either an overestimate of T_{eff} due to neglecting atmospheric effects caused by gas outflow (cf. 26, 147), or an underestimate of the opacity in the outer layers (cf. 243), or both. However, since star counts mostly reflect stellar lifetimes, the paucity of very bright O-type stars and the related problem of the O to WR star number ratio remain to be explained.

Bertelli et al. (26) suggested that in order to entirely reproduce the observed HR diagram together with the star frequencies, a modification to current radiative opacities in the region of the CNO ionization is unavoidable. In support of this idea, there are several independent arguments (121, 228) claiming that current opacity calculations may actually underestimate the true opacity in the middle temperature region (5×10^5 to 5×10^6 K), where the main sources are the bound-bound and bound-free transitions involving occupied levels of elements from carbon to iron. This does not mean that the old modification to radiative opacities, suggested long ago by Carson (39) and recently found to be inconsistent by Carson et al. (40) and Cox & Kidman (73), should be revived (cf. 242, 243, 245 for all details relative to models with Carson's opacity), but only that

current radiative opacities may underestimate the true stellar opacity in this particular range of temperature and density.

The evolution of binary stars has been studied in great detail by many authors (cf. 146, 147, 149 for very exhaustive reviews). Despite this, the effect of their presence on the frequencies of luminous stars in the various spectral types has not yet been fully assessed.

Finally, we recall the influence of rotation on stellar structure and evolution. This problem, in conjunction with the effects on stellar winds and internal mixing processes, has been addressed by many authors (cf. 221, 237, 254, and references quoted therein for more details). It certainly remains one of the most severe points of uncertainty and difficulty.

ACKNOWLEDGMENTS

We thank Drs. G. Bertelli and E. Nasi for useful discussions and great help in carefully reading the manuscript. We also express our gratitude to the National Council of Research of Italy (CNR-GNA-PSN) and National Swiss Foundation for Scientific Research for continued financial support.

Literature Cited

1. Abbott, D. C. 1978. *Ap. J.* 225–893
2. Abbott, D. C. 1979. In *Mass Loss and Evolution of O Type Stars*, ed. P. S. Conti, C. de Loore, p. 237. Dordrecht: Reidel
3. Abbott, D. C. 1980. *Ap. J.* 242: 1183
4. Abbott, D. C. 1982. *Ap. J.* 259: 282
5. Abbott, D. C. 1982. In *Wolf Rayet Stars: Observations, Physics, Evolution*, ed. C. de Loore, A. J. Willis, p. 185. Dordrecht: Reidel
6. Abbott, D. C. 1982. *Ap. J.* 263: 723
7. Abbott, D. C. 1985. In *O, Of and WR Stars*, ed. P. S. Conti, A. B. Underhill. NASA/CNRS Monogr. Ser. In press
8. Abbott, D. C., Bieging, J. H., Churchwell, E. B. 1981. *Ap. J.* 250: 645
9. Andriesse, C. D. 1979. *Astrophys. Space Sci.* 61: 205
10. Andriesse, C. D. 1980. *Astrophys. Space Sci.* 67: 461
11. Andriesse, C. D. 1980. *MNRAS* 192: 95
12. Appenzeller, I. 1980. In *Star Formation*, ed. A. Maeder, L. Martinet, p. 3. Geneva: Geneva Obs.
13. Appenzeller, I., Wolf, B. 1981. In *The Most Massive Stars*, ed. S. D'Odorico, D. Baade, K. Kjär, p. 131. Garching: ESO
14. Appenzeller, I. 1983. *Fundam. Cosmic Phys.* 7: 313
15. Appenzeller, I. 1985. In *Luminous Stars and Stellar Associations*, ed. P. S. Conti, C. de Loore, E. Kontizas. Dordrecht: Reidel. In press
16. Arnett, W. D. 1978. *Ap. J.* 219: 1008
17. Arnett, W. D., Thielemann, F. K. 1984. *MPA Rep. 90*, Max-Planck Inst., Garching, Fed. Rep. Germ.
18. Auré, J. L. 1971. *Astron. Astrophys.* 11: 345
19. Azzopardi, M., Breysacher, I. 1979. *Astron. Astrophys.* 75: 120
20. Barbaro, G., Bertelli, G., Chiosi, C., Nasi, E. 1973. *Astron. Astrophys.* 29: 185
21. Barlow, M. J. 1982. In *Wolf Rayet Stars: Observations, Physics, Evolution*, ed. C. de Loore, A. J. Willis, p. 149. Dordrecht: Reidel
22. Barlow, M. J., Cohen, M. 1977. *Ap. J.* 213: 737
23. Barlow, M. J., Hummer, D. G. 1982. In *Wolf Rayet Stars: Observations, Physics, Evolution*, ed. C. de Loore, A. J. Willis, p. 387. Dordrecht: Reidel
24. Barlow, M. J., Smith, L. J., Willis, A. J. 1981. *MNRAS* 196: 101
25. Bernat, A. P. 1977. *Ap. J.* 213: 756
26. Bertelli, G., Bressan, A., Chiosi, C. 1984. *Astron. Astrophys.* 130: 279
27. Bertelli, G., Bressan, A., Chiosi, C. 1985. *Astron. Astrophys.* 150: 33

28. Bertelli, G., Chiosi, C. 1981. In *The Most Massive Stars*, ed. S. D'Odorico, D. Baade, K. Kjär, p. 211. Garching: ESO
29. Bertelli, G., Chiosi, C. 1982. In *Wolf Rayet Stars: Observations, Physics, Evolution*, ed. C. de Loore, A. J. Willis, p. 359. Dordrecht: Reidel
30. Bond, J. R. 1984. In *Stellar Nucleosynthesis*, ed. C. Chiosi, A. Renzini, p. 297. Dordrecht: Reidel
31. Boury, A., Ledoux, P. 1965. *Ann. Astrophys.* 28: 353
32. Bressan, A., Bertelli, G., Chiosi, C. 1981. *Astron. Astrophys.* 102: 25
33. Breysacher, J. 1981. *Astron. Astrophys. Suppl.* 43: 203
34. Bruhweiler, F. C., Parsons, S. B., Wray, J. D. 1982. *Ap. J. Lett.* 256: L49
35. Brunish, W. M., Truran, J. W. 1982. *Ap. J.* 256: 247
36. Brunish, W. M., Truran, J. W. 1982. *Ap. J. Suppl.* 49: 447
37. Cahen, S. 1985. In *Nucleosynthesis and its Connection with Particle Physics*, ed. J. Audouze. Dordrecht: Reidel. In press
38. Cannon, C. J., Thomas, R. N. 1977. *Ap. J.* 211: 910
39. Carson, T. R. 1976. *Ann. Rev. Astron. Astrophys.* 14: 95
40. Carson, T. R., Huebner, W. F., Magee, N. H. Jr., Mertz, A. L. 1984. *Ap. J.* 283: 466
41. Cassinelli, J. P. 1979. *Ann. Rev. Astron. Astrophys.* 17: 275
42. Cassinelli, J. P., Olson, G. L., Stalio, R. 1978. *Ap. J.* 220: 573
43. Castor, J. I. 1981. In *Physical Processes in Red Giants*, ed. I. Iben Jr., A. Renzini, p. 285. Dordrecht: Reidel
44. Castor, J. I., Abbott, D. C., Klein, R. I. 1975. *Ap. J.* 195: 157
45. Chevalier, R. A. 1976. *Ap. J.* 208: 826
46. Chevalier, R. A. 1978. *Ann. NY Acad. Sci.* 302: 106
47. Chevalier, R. A. 1981. *Fundam. Cosmic Phys.* 7: 1
48. Chevalier, R. A., Kirshner, P. 1978. *Ap. J.* 219: 931
49. Chiosi, C. 1978. In *The HR Diagram*, ed. A. G. D. Philip, D. S. Hayes, p. 357. Dordrecht: Reidel
50. Chiosi, C. 1979. *Astron. Astrophys.* 80: 252
51. Chiosi, C. 1981. In *Effects of Mass Loss on Stellar Evolution*, ed. C. Chiosi, R. Stalio, p. 229. Dordrecht: Reidel
52. Chiosi, C. 1981. In *The Most Massive Stars*, ed. S. D'Odorico, D. Baade, K. Kjär, p. 27. Garching: ESO
53. Chiosi, C. 1981. *Astron. Astrophys.* 93: 163
54. Chiosi, C. 1982. In *Wolf Rayet Stars: Observations, Physics, Evolution*, ed. C. de Loore, A. J. Willis, p. 323. Dordrecht: Reidel
55. Chiosi, C., Caimmi, R. 1979. *Astron. Astrophys.* 80: 234
56. Chiosi, C., Greggio, L. 1980. *Astron. Astrophys.* 98: 336
57. Chiosi, C., Matteucci, F. 1984. In *Stellar Nucleosynthesis*, ed. C. Chiosi, A. Renzini, p. 333. Dordrecht: Reidel
58. Chiosi, C., Nasi, E. 1974. *Astron. Astrophys.* 34: 355
59. Chiosi, C., Nasi, E., Bertelli, G. 1979. *Astron. Astrophys.* 74: 62
60. Chiosi, C., Nasi, E., Sreenivasan, S. R. 1978. *Astron. Astrophys.* 63: 103
61. Chiosi, C., Summa, C. 1970. *Astrophys. Space Sci.* 8: 478
62. Cloutman, L. D. 1978. *Bull. Am. Astron. Soc.* 10: 400
63. Cloutman, L. D., Whitaker, R. 1980. *Ap. J.* 237: 900
64. Conti, P. S. 1976. *Mem. Soc. R. Sci. Liège, 6e Ser.* 9: 193
65. Conti, P. S. 1978. *Ann. Rev. Astron. Astrophys.* 16: 371
66. Conti, P. S. 1978. In *The HR Diagram*, ed. A. G. D. Philip, D. S. Hayes, p. 369. Dordrecht: Reidel
67. Conti, P. S. 1981. In *Effects of Mass Loss on Stellar Evolution*, ed. C. Chiosi, R. Stalio, p. 1. Dordrecht: Reidel
68. Conti, P. S. 1982. In *Wolf Rayet Stars: Observations, Physics, Evolution*, ed. C. de Loore, A. J. Willis, p. 3. Dordrecht: Reidel
69. Conti, P. S. 1984. In *Observational Tests of the Stellar Evolution Theory*, ed. A. Maeder, A. Renzini, p. 233. Dordrecht: Reidel
70. Conti, P. S., Garmany, C. D. 1980. *Ap. J.* 238: 190
71. Conti, P. S., Garmany, C. D., de Loore, C., Vanbeveren, D. 1983. *Ap. J.* 274: 302
72. Conti, P. S., Leep, E. M., Perry, D. N. 1983. *Ap. J.* 268: 228
73. Cox, A. N., Kidman, R. B. 1984. In *Observational Tests of the Stellar Evolution Theory*, ed. A. Maeder, A. Renzini, p. 41. Dordrecht: Reidel
74. Czerny, M. 1979. *Acta Astron.* 29: 1
75. Dallaporta, N. 1971. In *Colloquium on Supergiant Stars*, ed. M. Hack, p. 250. Trieste: Trieste Obs.
76. Davidson, K., Dufour, R. J., Walborn, N. R., Gull, T. R. 1984. In *Observational Tests of the Stellar Evolution Theory*, ed. A. Maeder, A. Renzini, p. 261. Dordrecht: Reidel
77. Davidson, K., Walborn, N. R., Gull, T. R. 1982. *Ap. J. Lett.* 254: L47

78. Dearborn, D. S. P., Blake, J. B. 1979. *Ap. J.* 231: 193
79. Dearborn, D. S. P., Blake, J. B., Hainebach, K. L., Schramm, D. N. 1978. *Ap. J.* 223: 552
80. Dearborn, D. S. P., Eggleton, P. P. 1977. *Ap. J.* 213: 448
81. Doom, C. 1982. *Astron. Astrophys.* 116: 303
82. Doom, C. 1982. *Astron. Astrophys.* 116: 308
83. Doom, C. 1984. *Astron. Astrophys.* 138: 101
84. Doom, C., De Greve, J. P., de Loore, C. 1985. *Ap. J.* 290: 185
85. Dupree, A. K. 1981. In *Effects of Mass Loss on Stellar Evolution*, ed. C. Chiosi, R. Stalio, p. 87. Dordrecht: Reidel
86. El Eid, M. F., Fricke, K. J., Ober, W. W. 1983. *Astron. Astrophys.* 119: 54
87. Falk, H. J., Mitalas, R. 1981. *MNRAS* 196: 225
88. Firmani, C. 1982. In *Wolf Rayet Stars: Observations, Physics, Evolution*, ed. C. de Loore, A. J. Willis, p. 499. Dordrecht: Reidel
89. Fowler, W. A., Caughlan, G. R., Zimmerman, B. A. 1975. *Ann. Rev. Astron. Astrophys.* 13: 69
90. Freedman, W. 1985. In *Spectral Evolution of Galaxies*, ed. C. Chiosi, A. Renzini, p. 183. Dordrecht: Reidel
91. Fusi-Pecci, F., Renzini, A. 1976. *Astron. Astrophys.* 46: 447
92. Gabriel, M. 1969. *Astron. Astrophys.* 1: 321
93. Gabriel, M., Noels, A. 1976. *Astron. Astrophys.* 53: 149
94. Garmany, C. D., Conti, P. S., Chiosi, C. 1982. *Ap. J.* 263: 777
95. Garmany, C. D., Conti, P. S. 1984. *Ap. J.* 284: 705
96. Garmany, C. D., Conti, P. S. 1985. *Ap. J.* 293: 407
97. Garmany, C. D., Massey, P., Conti, P. S. 1984. *Ap. J.* 278: 233
98. Garmany, C. D., Olson, G. L., Conti, P. S., Van Steenberg, M. E. 1981. *Ap. J.* 250: 660
99. Giannone, P., Kohl, K., Weigert, A. 1968. *Z. Astrophys.* 68: 107
100. Goldberg, L. 1979. *Q. J. R. Astron. Soc.* 20: 361
101. Greggio, L. 1984. In *Observational Tests of the Stellar Evolution Theory*, ed. A. Maeder, A. Renzini, p. 329. Dordrecht: Reidel
102. Hagen, W. 1978. *Ap. J. Suppl.* 38: 1
103. Hartwick, F. D. A. 1967. *Ap. J.* 150: 953
104. Hearn, A. G. 1981. In *Effects of Mass Loss on Stellar Evolution*, ed. C. Chiosi, R. Stalio, p. 125. Dordrecht: Reidel
105. Hellings, P., Vanbeveren, D. 1981. *Astron. Astrophys.* 95: 14
106. van den Heuvel, E. P. J. 1976. In *Structure and Evolution of Close Binary Systems*, ed. P. Eggleton, S. Mitton, J. Whelau, p. 35. Dordrecht: Reidel
107. van den Heuvel, E. P. J., Habets, G. M. H. J. 1984. *Nature* 309: 598
108. van den Heuvel, E. P. J., Heize, J. 1972. *Nature Phys. Sci.* 239: 67
109. Hidayat, B., Admiranto, A. G., van der Hucht, K. A. 1984. *Astrophys. Space Sci.* 99: 175
110. Hidayat, B., Supelli, K., van der Hucht, K. A. 1982. In *Wolf Rayet Stars: Observations, Physics, Evolution*, ed. C. de Loore, A. J. Willis, p. 27. Dordrecht: Reidel
111. van der Hucht, K. A., Conti, P. S., Lundstrom, I., Stenholm, B. 1981. *Space Sci. Rev.* 28: 227
112. van der Hucht, K. A., Bernat, A. P., Kondo, Y. 1980. *Astron. Astrophys.* 82: 14
113. Humphreys, R. M. 1982. In *The Most Massive Stars*, ed. S. D'Odorico, D. Baade, K. Kjär, p. 5. Garching: ESO
114. Humphreys, R. M. 1984. In *Observational Tests of the Stellar Evolution Theory*, ed. A. Maeder, A. Renzini, p. 279. Dordrecht: Reidel
115. Humphreys, R. M. Davidson, K. 1979. *Ap. J.* 232: 409
116. Humphreys, R. M., McElroy, D. B. 1984. *Ap. J.* 284: 565
117. Humphreys, R. M., Nichols, M., Massey, P. 1985. *Astron. J.* 90: 101
118. Hutchings, J. B. 1982. *Ap. J.* 255: 70
119. Iben, I. Jr. 1974. *Ann. Rev. Astron. Astrophys.* 12: 215
120. Iben, I. Jr., Renzini, A. 1983. *Ann. Rev. Astron. Astrophys.* 21: 271
121. Iben, I. Jr., Renzini, A. 1984. *Phys. Rep.* 105(6): 329
122. de Jager, C. 1980. *The Bright Stars.* Dordrecht: Reidel
123. de Jager, C. 1984. *Astron. Astrophys.* 138: 246
124. de Jager, C., Nieuwenhuijzen, H., van der Hucht, K. A. 1985. In *Luminous Stars and Stellar Associations*, ed. P. S. Conti, C. de Loore, E. Kontizas. Dordrecht: Reidel. In press
125. Johnston, M. D., Yahil, A. 1984. *Ap. J.* 285: 587
126. Kato, S. 1966. *Publ. Astron. Soc. Jpn.* 18: 374
127. Kettner, K. U., Becker, H. W., Buchman, L., Gorres, J., Kravinkel, H., et al. 1982. *Z. Phys.* 308: 73
128. Kippenhahn, R., Weigert, A. 1967. *Z. Astrophys.* 65: 251
129. Kirbiyik, H., Bertelli, G., Chiosi, C.

1984. In *Theoretical Problems in Stellar Stability and Oscillations, Liège Int. Conf., 25th*, p. 126. Liège: Inst. Astrophys.
130. Kudritzki, R. P. 1985. In *Luminous Stars and Stellar Associations*, ed. P. S. Conti, C. de Loore, E. Kontizas. Dordrecht: Reidel. In press
131. Kunth, D., Sargent, W. L. W. 1973. *Ap. J.* 273: 81
132. Kwok, S. 1980. *J. R. Astron. Soc. Can.* 47: 216
133. Kwok, S. 1984. In *Relations Between Chromospheric Coronal Heating and Mass Loss in Stars, Trieste Workshop, 3rd.* In press
134. Lamb, S. A. 1978. *Ap. J.* 220: 186
135. Lamb, S. A., Iben, I. Jr., Howard, W. M. 1976. *Ap. J.* 207: 209
136. Lamers, H. J. G. L. M. 1981. *Ap. J.* 245: 593
137. Lamers, H. J. G. L. M. 1985. In *Luminous Stars and Stellar Associations*, ed. P. S. Conti, C. de Loore, E. Kontizas. Dordrecht: Reidel. In press
138. Lamers, H. J. G. L. M., Paerels, F., de Loore, C. 1980. *Astron. Astrophys.* 87: 68
139. Lamers, H. J. G. L. M., de Groot, M., Cassatella, A. 1983. *Astron. Astrophys.* 123: L8
140. Lamers, H. J. G. L. M., Rogerson, J. B. Jr. 1978. *Astron. Astrophys.* 66: 417
141. Langanke, K., Koonin, S. E. 1982. *Nucl. Phys. A* 410: 334
142. Lauterborn, D., Refsdal, S., Weigert, A. 1971. *Astron. Astrophys.* 10: 97
143. Ledoux, P. 1947. *Ap. J.* 94: 537
144. Linsky, J. L. 1981. In *Effects of Mass Loss on Stellar Evolution*, ed. C. Chiosi, R. Stalio, p. 187. Dordrecht: Reidel
145. de Loore, C. 1980. *Space Sci. Rev.* 26: 113
146. de Loore, C. 1981. In *Effects of Mass Loss on Stellar Evolution*, ed. C. Chiosi, R. Stalio, p. 405. Dordrecht: Reidel
147. de Loore, C. 1982. In *Wolf Rayet Stars: Observations, Physics, Evolution*, ed. C. de Loore, A. J. Willis, p. 343. Dordrecht: Reidel
148. de Loore, C. 1984. *Phys. Scr.* T7: 25
149. de Loore, C. 1984. In *Observational Tests of the Stellar Evolution Theory*, ed. A. Maeder, A. Renzini, p. 251. Dordrecht: Reidel
150. de Loore, C., De Greve, J. P., De Cuyper, J. P. 1975. *Astrophys. Space Sci.* 36: 219
151. de Loore, C., De Greve, J. P., Lamers, H. J. G. L. M. 1977. *Astron. Astrophys.* 61: 251
152. de Loore, C., De Greve, J. P., Vanbeveren, D. 1978. *Astron. Astrophys.* 67: 373
153. de Loore, C., Hellings, P., Lamers, H. J. G. L. M. 1982. In *Wolf Rayet Stars: Observations, Physics, Evolution*, ed. C. de Loore, A. J. Willis, p. 53. Dordrecht: Reidel
154. Lovy, D., Maeder, A., Noels, A., Gabriel, M. 1984. *Astron. Astrophys.* 133: 307
155. Lucy, L. B., Solomon, P. M. 1970. *Ap. J.* 159: 879
156. Lucy, L. B., White, R. L. 1980. *Ap. J.* 241: 300
157. Maeder, A. 1975. *Astron. Astrophys.* 40: 303
158. Maeder, A. 1976. *Astron. Astrophys.* 47: 384
159. Maeder, A. 1980. *Astron. Astrophys.* 90: 311
160. Maeder, A. 1980. *Astron. Astrophys.* 92: 101
161. Maeder, A. 1981. In *The Most Massive Stars*, ed. S. D'Odorico, D. Baade, K. Kjär, p. 173. Garching: ESO
162. Maeder, A. 1981. *Astron. Astrophys.* 99: 97
163. Maeder, A. 1981. *Astron. Astrophys.* 102: 401
164. Maeder, A. 1981. *Astron. Astrophys.* 101: 385
165. Maeder, A. 1982. *Astron. Astrophys.* 105: 149
166. Maeder, A. 1983. *Astron. Astrophys.* 120: 113
167. Maeder, A. 1983. In *Primordial Helium*, ed. P. A. Shaver, D. Kunth, K. Kjär, p. 89. Garching: ESO
168. Maeder, A. 1984. In *Stellar Nucleosynthesis*, ed. C. Chiosi, A. Renzini, p. 115. Dordrecht: Reidel
169. Maeder, A. 1984. In *Observational Tests of the Stellar Evolution Theory*, ed. A. Maeder, A. Renzini, p. 299. Dordrecht: Reidel
170. Maeder, A. 1985. *Astron. Astrophys.* 147: 300
171. Maeder, A. 1986. *Astron. Astrophys.* In press
172. Maeder, A., Lequeux, J. 1982. *Astron. Astrophys.* 114: 409
173. Maeder, A., Lequeux, J., Azzopardi, M. 1980. *Astron. Astrophys.* 90: L17
174. Maeder, A., Mermilliod, J. C. 1981. *Astron. Astrophys.* 93: 136
175. Mallik, D. C. W. 1980. *Astrophys. Space Sci.* 69: 133
176. Mallik, D. C. W. 1981. *J. Astrophys. Astron.* 2: 171
177. Massevich, A. G., Tutukov, A. V. 1973. In *Late Stages of Stellar Evolution*, ed. R. J. Tayler, p. 73. Dordrecht: Reidel
178. Massey, P. 1980. *Ap. J.* 336: 526

179. Massey, P. 1981. *Ap. J.* 246: 153
180. Massey, P. 1982. In *Wolf Rayet Stars: Observations, Physics, Evolution*, ed. C. de Loore, A. J. Willis, p. 387. Dordrecht: Reidel
181. Massey, P., Conti, P. S. 1980. *Ap. J.* 242: 638
182. Massey, P., Conti, P. S., Niemela, V. S. 1981. *Ap. J.* 246: 145
183. Matraka, B., Wassermann, C., Weigert, A. 1982. *Astron. Astrophys.* 107: 283
184. Merrill, K. M. 1978. In *The Interaction of Variable Stars With Their Environment*, ed. R. Kippenhahn, J. Rahe, W. Strohmeir, p. 446. Dordrecht: Reidel
185. Metzger, P. 1976. *Proc. Eur. Astron. Meet., 3rd, Tbilisi*, ed. E. K. Kharadze, p. 369
186. Metzger, P., Gusten, R. 1983. *Vistas Astron.* 26(3): 159
187. Meylan, G., Maeder, A. 1982. *Astron. Astrophys.* 108: 148
188. Meylan, G., Maeder, A. 1983. *Astron. Astrophys.* 124: 84
189. Moffat, A. F. J. 1981. In *Effects of Mass Loss on Stellar Evolution*, ed. C. Chiosi, R. Stalio, p. 301. Dordrecht: Reidel
190. Moran, J. M. 1976. In *Frontiers of Astrophysics*, ed. E. H. Avrett, p. 385. Cambridge: Cambridge Univ. Press
191. Nasi, E. 1985. In *Luminous Stars and Stellar Associations*, ed. P. S. Conti, C. de Loore, E. Kontizas. Dordrecht: Reidel. In press
192. Nelson, G. D., Hearn, A. G. 1978. *Astron. Astrophys.* 65: 223
193. Niemela, V. S. 1981. In *Effects of Mass Loss on Stellar Evolution*, ed. C. Chiosi, R. Stalio, p. 307. Dordrecht: Reidel
194. Niemela, V. S., Conti, P. S., Massey, P. 1980. *Ap. J.* 241: 1050
195. Noels, A., Conti, P. S., Gabriel, M., Vreux, J. M. 1980. *Astron. Astrophys.* 92: 242
196. Noels, A., Gabriel, M. 1981. *Astron. Astrophys.* 101: 215
197. Noels, A., Magain, E. 1984. *Astron. Astrophys.* 139: 341
198. Noels, A., Maserel, C. 1982. *Astron. Astrophys.* 105: 293
199. Nomoto, K. 1984. In *Stellar Nucleosynthesis*, ed. C. Chiosi, A. Renzini, p. 205. Dordrecht: Reidel
200. Nugis, T. 1975. In *Variable Stars and Stellar Evolution*, ed. V. E. Sherwood, L. Plaut, p. 291. Dordrecht: Reidel
201. Nugis, T. 1982. In *Wolf Rayet Stars: Observations, Physics, Evolution*, ed. C. de Loore, A. J. Willis, p. 127. Dordrecht: Reidel
202. Nussbaumer, H., Schmutz, W., Smith, L. J., Willis, A. J. 1982. *Astron. Astrophys. Suppl.* 47: 257
203. Paerels, F. B. S., Lamers, H. J. G. L. M., de Loore, C. 1980. *Astron. Astrophys.* 90: 204
204. Peimbert, M., van den Bergh, S. 1971. *Ap. J.* 167: 233
205. Peimbert, M., Torres-Peimbert, S. 1976. *Ap. J.* 203: 581
206. Peimbert, M., Torres-Peimbert, S. 1977. *MNRAS* 179: 217
207. Pylyser, E., Doom, C., de Loore, C. 1985. *Astron. Astrophys.* 148: 379
208. Reimers, D. 1973. *Astron. Astrophys.* 24: 79
209. Reimers, D. 1975. *Mem. Soc. R. Sci. Liège, 6e Ser.* 8: 369
210. Reimers, D. 1977. *Astron. Astrophys.* 57: 395
211. Reimers, D. 1978. In *The Interaction of Variable Stars With Their Environment*, ed. R. Kippenhahn, J. Rahe, W. Strohmeir, p. 559. Dordrecht: Reidel
212. Reimers, D. 1981. In *Physical Processes in Red Giants*, ed. I. Iben Jr., A. Renzini, p. 269. Dordrecht: Reidel
213. Renzini, A. 1984. In *Observational Tests of the Stellar Evolution Theory*, ed. A. Maeder, A. Renzini, p. 21. Dordrecht: Reidel
214. Renzini, A., Voli, M. 1981. *Astron. Astrophys.* 94: 175
215. Roxburgh, I. 1978. *Astron. Astrophys.* 65: 281
216. Sakashita, S., Hayashi, C. 1958. *Prog. Theor. Phys.* 22: 830
217. Sakashita, S., Hayashi, C. 1961. *Prog. Theor. Phys.* 26: 942
218. Sanner, F. 1976. *Ap. J.* 204: 141
219. Saslaw, W. C., Schwarzschild, M. 1965. *Ap. J.* 142: 1468
220. Scalo, J. 1986. *Fundam. Cosmic Phys.* In press
221. Schatzman, E. 1984. In *Observational Tests of the Stellar Evolution Theory*, ed. A. Maeder, A. Renzini, p. 491. Dordrecht: Reidel
222. Schild, H., Maeder, A. 1984. *Astron. Astrophys.* 136: 237
223. Schild, H., Maeder, A. 1985. *Astron. Astrophys.* 143: L7
224. Schmutz, W. 1982. In *Wolf Rayet Stars: Observations, Physics, Evolution*, ed. C. de Loore, A. J. Willis, p. 387. Dordrecht: Reidel
225. Schönberner, D. 1979. *Astron. Astrophys.* 79: 108
226. Schwarzschild, M., Härm, R. 1958. *Ap. J.* 128: 348
227. Shaviv, G., Salpeter, E. E. 1973. *Ap. J.* 184: 191
228. Simon, N. R. 1982. *Ap. J. Lett.* 260: L87

229. Simon, N. R., Stothers, R. 1969. *Ap. J.* 155: 247
230. Simon, N. R., Stothers, R. 1970. *Astron. Astrophys.* 6: 183
231. Simpson, E. 1971. *Ap. J.* 165: 295
232. Smith, L. F. 1973. In *WR and High Temperature Stars*, ed. M. K. V. Bappu, J. Sahade, p. 15. Dordrecht: Reidel
233. Smith, L. F. 1982. In *Wolf Rayet Stars: Observations, Physics, Evolution*, ed. C. de Loore, A. J. Willis, p. 597. Dordrecht: Reidel
234. Smith, L. J., Willis, A. J. 1982. *MNRAS* 201: 451
235. Sreenivasan, S. R., Wilson, W. J. F. 1978. *Astrophys. Space Sci.* 30: 57
236. Sreenivasan, S. R., Wilson, W. J. F. 1982. *Ap. J.* 254: 287
237. Sreenivasan, S. R., Wilson, W. J. F. 1985. *Ap. J.* 292: 506
238. Stahl, O., Wolf, B., Klare, G., Cassatella, J., Krautter, J., et al. 1983. *Astron. Astrophys.* 127: 49
239. Stencel, R. E. 1978. *Ap. J. Lett.* 223: L37
240. Stothers, R. 1970. *MNRAS* 151: 65
241. Stothers, R., Chin, C. W. 1976. *Ap. J.* 204: 472
242. Stothers, R., Chin, C. W. 1976. *Ap. J.* 209: 800
243. Stothers, R., Chin, C. W. 1977. *Ap. J.* 211: 189
244. Stothers, R., Chin, C. W. 1978. *Ap. J.* 226: 231
245. Stothers, R., Chin, C. W. 1978. *Ap. J.* 225: 939
246. Stothers, R., Chin, C. W. 1979. *Ap. J.* 233: 267
247. Stothers, R., Chin, C. W. 1980. *Ap. J.* 240: 885
248. Stothers, R., Chin, C. W. 1981. *Ap. J.* 247: 1063
249. Stothers, R., Chin, C. W. 1983. *Ap. J.* 264: 583
250. Stothers, R., Chin, C. W. 1985. *Ap. J.* 292: 222
251. Stothers, R., Simon, N. R. 1970. *Ap. J.* 160: 1019
252. Tanaka, Y. 1966. *Publ. Astron. Soc. Jpn.* 18: 47
253. Tanaka, Y. 1966. *Prog. Theor. Phys.* 36: 844
254. Tassoul, J. L. 1984. In *Observational Tests of the Stellar Evolution Theory*, ed. A. Maeder, A. Renzini, p. 475. Dordrecht: Reidel
255. Thielemann, F. K., Arnett, W. D. 1984. *MPA Rep. 91*, Max-Planck Inst., Garching, Fed. Rep. Germ.
256. Tinsley, B. M. 1980. *Fundam. Cosmic Phys.* 5: 287
257. Underhill, A. B. 1980. *Ap. J.* 239: 220
258. Underhill, A. B. 1981. *Ap. J.* 244: 963
259. Underhill, A. B. 1983. *Ap. J.* 265: 933
260. Underhill, A. B. 1983. *Ap. J.* 266: 718
261. Vanbeveren, D. 1985. In *Luminous Stars and Stellar Associations*, ed. P. S. Conti, C. de Loore, E. Kontizas. Dordrecht: Reidel. In press
262. Vanbeveren, D., Conti, P. S. 1980. *Astron. Astrophys.* 80: 230
263. Vanbeveren, D., de Loore, C. 1980. *Astron. Astrophys.* 86: 21
264. Varshawsky, V. I., Tutukov, A. V. 1973. *Nauch. Inform. Acad. Nauk.* 26: 35
265. Waldron, W. L. 1984. In *The Origin of Non-Radiative Heating/Momentum in Hot Stars*, ed. A. B. Underhill, A. G. Michalitsianos, p. 2358. Washington: NASA
266. Willis, A. J. 1980. *Proc. Eur. IUE Conf., 2nd, Tubingen*, p. i1
267. Willis, A. J. 1982. In *Wolf Rayet Stars: Observations, Physics, Evolution*, ed. C. de Loore, A. J. Willis, p. 87. Dordrecht: Reidel
268. Willis, A. J. 1983. In *Wolf Rayet Stars: Progenitors of Supernovae*, ed. M. C. Lortet, A. Pitault, p. VII. 3. Meudon: Meudon Obs.
269. Willis, A. J., Wilson, R. 1978. *MNRAS* 182: 559
270. Wilson, I. R. G., Dopita, M. A. 1985. *Astron. Astrophys.* 149: 295
271. Wilson, J. R., Mayle, J., Woosley, S. E., Weaver, T. A. 1985. *Proc. Tex. Symp., 12th.* In press
272. Woosley, S. E., Axelrod, T. S., Weaver, T. A. 1984. In *Stellar Nucleosynthesis*, ed. C. Chiosi, A. Renzini, p. 263. Dordrecht: Reidel
273. Woosley, S. E., Weaver, T. A. 1983. In *Supernovae: A Survey of Current Research*, ed. M. J. Rees, J. Stoneham, p. 79. Dordrecht: Reidel
274. Ziolkowski, J. 1972. *Acta Astron.* 22: 327